

**MODELING AND ANALYSIS OF ELECTRICAL
SYSTEM FOR OFFSHORE OIL AND GAS
PLATFORM**

ELISABETH ØEN

SUPERVISOR
Rade Ciric

University of Agder, 2023
Faculty of Engineering and Science
Department of Engineering and Sciences

Master

Obligatorisk gruppeerklæring

Den enkelte student er selv ansvarlig for å sette seg inn i hva som er lovlige hjelpemidler, retningslinjer for bruk av disse og regler om kildebruk. Erklæringen skal bevisstgjøre studentene på deres ansvar og hvilke konsekvenser fusk kan medføre. Manglende erklæring fritar ikke studentene fra sitt ansvar.

1.	Jeg erklærer herved at vår besvarelse er vårt eget arbeid, og at vi ikke har brukt andre kilder eller har mottatt annen hjelp enn det som er nevnt i besvarelsen.	Ja
2.	Jeg erklærer videre at denne besvarelsen: <ul style="list-style-type: none">• Ikke har vært brukt til annen eksamen ved annen avdeling/universitet/høgskole innenlands eller utenlands.• Ikke refererer til andres arbeid uten at det er oppgitt.• Ikke refererer til eget tidligere arbeid uten at det er oppgitt.• Har alle referansene oppgitt i litteraturlisten.• Ikke er en kopi, duplikat eller avskrift av andres arbeid eller besvarelse.	Ja
3.	Jeg er kjent med at brudd på ovennevnte er å betrakte som fusk og kan medføre annullering av eksamen og utestengelse fra universiteter og høgskoler i Norge, jf. Universitets- og høgskoleloven §§4-7 og 4-8 og Forskrift om eksamen §§ 31.	Ja
4.	Jeg er kjent med at alle innleverte oppgaver kan bli plagiatkontrollert.	Ja
5.	Jeg er kjent med at Universitetet i Agder vil behandle alle saker hvor det forligger mistanke om fusk etter høgskolens retningslinjer for behandling av saker om fusk.	Ja
6.	Jeg har satt oss inn i regler og retningslinjer i bruk av kilder og referanser på biblioteket sine nettsider.	Ja

Publiseringsavtale

Fullmakt til elektronisk publisering av oppgaven Forfatter(ne) har opphavsrett til oppgaven. Det betyr blant annet enerett til å gjøre verket tilgjengelig for allmennheten (Åndsverkloven. §2).

Oppgaver som er unntatt offentlighet eller taushetsbelagt/konfidensiell vil ikke bli publisert.

Vi gir herved Universitetet i Agder en vederlagsfri rett til å gjøre oppgaven tilgjengelig for elektronisk publisering:	Ja
Er oppgaven båndlagt (konfidensiell)?	Nei
Er oppgaven unntatt offentlighet?	Nei

Acknowledgements

This thesis is the final submission of my master's degree in Renewable Energy at the University of Agder. I have previously completed a bachelor's degree in Electrical Power Engineering at NTNU, Trondheim, where my interest for power system analysis started. Thank you to Rade Ciric for saying yes to being my supervisor.

I would like to take this opportunity to thank Aker Solutions and Aker BP for letting me write my master's thesis for them about Valhall PWP and for providing me with data and information. Especially thanks to Ian Gore and Julia Yang for being my main helpers from Aker Solutions. Also, I would like to thank Hans Anders Faraasen from Unitech for helping me with the model in DIgSILENT PowerFactory.

The software PowerFactory by DIgSILENT was completely new to me and I have had a lot of struggles with running the system. This has caused me to reduce the scope of work compared to what was intended to do, which is unfortunate. Nevertheless, I have learned a lot about modeling and analysis of a power system, especially about short-circuit currents throughout this semester.

June 2023
Grimstad, Norway

Elisabeth Øen

Abstract

The main objective of power system analysis is to ensure that the electrical power system is modeled in a safe, reliable, and efficient manner. Short-circuit analysis is a power system analysis investigating the maximum and minimum currents during a fault or short-circuit.

The power system analysis software PowerFactory by DIgSILENT was used for modeling and analyzing an 11kV offshore oil and gas platform that is powered from shore through an HVDC cable. Short-circuit analysis according to IEC 60909 was conducted for various combinations of open and closed bus-ties between the 690V switchboards or the 11kV switchboards under normal operation mode. Maximum and minimum short-circuit currents were considered to ensure compliance with switchgear ratings and protective device coordination. The results display short-circuit currents within defined limits, indicating the electrical network is modeled safely and reliably. For further work, it is recommended to develop the electrical model further by doing analysis for other operation types, like essential and emergency operations, and conducting other power system analyses, for instance, arc flash analysis and load flow.

Sammendrag

Kraftsystemanalyser er en vesentlig del av elektrisk kraftsystemdesign og har som hovedmål å sikre at det elektriske kraftsystemet modelleres på en sikker, pålitelig og effektiv måte. Kortslutningsanalyse er en kraftsystemanalyse som undersøker de maksimale og minimale strømmene under en feil eller kortslutning.

Programvaren PowerFactory fra DlgSILENT ble brukt til å modellere og analysere en 11 kV offshore olje- og gassplattform som blir forsynt fra land via en likestrøms kabel. Kortslutningsanalyse i henhold til IEC 60909 ble utført for ulike kombinasjoner av åpne og lukkede brytere mellom 690 V tavler eller 11 kV tavler under normal driftsmodus. Maksimale og minimale kortslutningsstrømmer ble vurdert for å sikre overholdelse av vern- og beskyttelsesutstørs spesifikasjoner. Resultatene viser kortslutningsstrømmer innenfor definerede grenser, noe som indikerer at det elektriske nettverket er modellert på en trygg og pålitelig måte.

For videre arbeid anbefales det å videreutvikle den elektriske modellen ved å utføre analyser for andre driftstyper, som for eksempel essensielle og nødsituasjoner, samt å utføre andre kraftsystemanalyser, for eksempel lysbueanalyse og lastflytanalyse.

Contents

Acknowledgements	ii
Abstract	iv
Sammendrag	v
List of Figures	ix
List of Tables	xi
Nomenclature and Abbreviations	xiii
1 Introduction	1
1.1 Background	1
1.1.1 The Valhall Field	2
1.2 Contribution	3
1.3 Objectives	3
1.4 Limitations	3
1.5 Structure	4
2 Literature Review	5
3 Theory	7
3.1 Short-Circuit	7
3.1.1 Standards	9
3.1.2 IEC 60909	10
3.1.3 Impedances, Z	11
3.1.4 Initial Symmetrical Short-Circuit Current, I_k''	12
3.1.5 Peak Short-Circuit Current, i_p	12
3.1.6 Symmetrical Short-Circuit Breaking Current, I_b	13
3.1.7 DC-Component of the Short-Circuit Current, i_{DC}	14
3.1.8 Steady-State Short-Circuit Current, I_k	14
3.2 Electrical Arc	15
3.2.1 Arcing in Cubicle	15
3.2.2 Arc Flash	16
3.2.3 IEEE 1584	16
3.2.4 PPE	19
4 Methods	21
4.1 Collection of Data	21
4.2 Modeling in DIgSILENT PowerFactory	21
4.2.1 High Voltage System	22
4.2.2 Low Voltage System	23
4.2.3 PFS Modeling	24

4.2.4	Breaking and Making Capacity	25
4.2.5	Minimum Short-Circuit	25
4.3	Case Study	26
4.4	Short-Circuit Calculation	28
4.5	Arc-Flash Analysis	29
5	Results and Discussions	31
5.1	Short-Circuit Currents	31
5.1.1	Maximum Short-Circuit Currents	31
5.1.2	Discussion of the Maximum Short-Circuit Results	33
5.1.3	Minimum Short-Circuit Currents	34
5.1.4	Discussion of the Minimum Short-Circuit Results	35
6	Conclusions and Further Work	37
	Bibliography	38
A	Coefficients for arc-flash hazard analysis	40
A.1	Coefficients for calculating arcing current	40
A.2	Coefficients for calculating incident energy	40
	Appendix	40

List of Figures

1.1	Location of the Valhall oil field on the Norwegian Continental Shelf (NCS) [3]	2
1.2	Illustration of the Valhall field and the platforms	3
3.2	Short-circuit types according to IEC 60909 [8] [17]	9
3.3	Comparison of two methods for short-circuit calculations [16]	10
3.4	Equivalent circuit diagram for a network with transformer [8]	10
3.5	Short-circuit current as a function of time with decaying AC component [16]	11
3.6	The value κ to the R/X- or X/R-ratio [8]	13
3.7	Graphs for determining μ and q for calculation of I_b [8]	14
3.8	The principle behind an electrical arc [20]	15
3.9	The stages of arc formation in a cubicle [7]	15
3.10	Electrode configurations [23]	17
3.11	Protective Clothing according to NFPA 70E [14]	19
4.1	Electrical model	22
A.1	Coefficients for Equation 3.21 [9]	40
A.2	Coefficients for Equation 3.22 [9]	40

List of Tables

3.1	Voltage factor, c, for calculating the minimum and maximum short-circuit currents	11
3.2	Typical bus gaps and enclosure size for different equipment classes [9]	17
3.3	Typical working distance different equipment classes	18
4.1	Different switchboards located on the platform	21
4.2	HV transformer data	22
4.3	High Voltage Main Cables	23
4.4	LV transformer data	24
4.5	Low Voltage Main Cables	24
4.6	Breaking and making capacities for the different voltage-levels	25
4.7	NORSOK E-001:2016 requirements for maximum I_k''	25
4.8	Rated current to be compared with minimum short-circuit calculations	25
4.9	Calculation settings for maximum short-circuit	28
4.10	Calculation settings for minimum short-circuit	28
4.11	Switchboard design	29
4.12	Circuit breakers and respective fault clearing time	29
4.13	Arc flash protection for 11kV and 690V switchboards	29
5.1	Results from case 1	31
5.2	Results from case 2	31
5.3	Results from case 3	32
5.4	Results from case 4	32
5.5	Results from case 5	33
5.6	Results from case 6	33
5.7	Results from case 7	34
5.8	Results from case 8	34
5.9	Results from case 9	34
5.10	Results from case 10	35

Nomenclature and Abbreviations

I_b Short-circuit breaking current.

I_k Steady-state short-circuit current.

I_k'' Initial symmetrical short-circuit current.

I_{rT} Rated current of transformer.

I_r Rated current.

P_{krT} Total loss in the windings of transformer at rated current.

S_{rT} Rated apparent power of transformer.

U_n Nominal voltage of the network.

U_{rT} Rated voltage of transformer.

V_{OC} Open-circuit voltage.

i_{DC} Aperiodic component of the instantaneous current.

i_p Peak short-circuit current.

t_k Duration of short-circuit.

u_{Rr} Rated resistive component of a transformer.

u_{kr} Rated short circuit voltage of a transformer.

z_0 Zero sequence impedance.

z_1 Positive sequence impedance.

AC Alternating current.

AN Air Natural.

c-factor Safety factor.

DC Direct current.

FEED Front-end engineering design.

GHG Greenhouse gas.

HV High Voltage.

HVDC High Voltage Direct Current.

IEC International Electrotechnical Commission.

IP Injection Platform.

LV Low Voltage.

NCS Norwegian Continental Shelf.

PFS Power From Shore.

PH Production and Housing.

PPE Personal Protective Equipment.

PWP Production and Wellhead Platform.

UI Unmanned Installation.

VFN Valhall Flank North.

VFS Valhall Flank South.

VFW Valhall Flank West.

WP Wellhead Platform.

Chapter 1

Introduction

In this chapter, the introduction will be presented, including background, objectives, limitations, and the structure of the thesis.

1.1 Background

Norway, renowned as one of the world's leading oil and gas nations, has greatly benefited from its oil resources, contributing to its wealth. However, the oil and gas sector in Norway is responsible for a significant portion, approximately 25%, of the country's Greenhouse gas (GHG) emissions [1]. Conventionally, offshore oil and gas platforms have relied on gas turbines for power generation, which accounts for a major portion of the emissions as well as having low efficiencies.

Given the current climate crisis and the global emphasis on renewable and clean energy sources, there is a growing need to reduce emissions and carbon footprint in the oil and gas industry. One strategy for reducing emissions is to power the platform from shore, just like the platform considered in this master thesis: PWP on the Valhall field.

Oil and gas platforms are complex facilities and are dependent on safe and reliable systems, including the electrical system. Oil and gas platforms are exposed to demanding conditions, like explosive atmospheres and hazardous gases, and the consequences of an electrical fault, like short-circuits and arc-flashes, can pose a risk for both equipment and personnel. By prioritizing accurate short circuit calculations and thorough arc flash analyses on oil and gas platforms, operators can effectively mitigate the risks associated with electrical faults. This proactive approach not only protects personnel from potential injuries but also safeguards critical equipment, and minimizes costly downtime. Ultimately, incorporating these calculations and analysis into the design, maintenance, and safety planning of electrical systems on oil and gas platforms contributes to safer operations, increased reliability, and improved overall performance.

1.1.1 The Valhall Field

Valhall is a Norwegian oil field located in the southern part of the Norwegian Continental shelf, NCS, and has been in production since 1982. Figure 1.1 shows the location of Valhall on the NCS. The field is operated by Aker BP and is for the moment undergoing a modernizing phase where some old platforms are removed as well as planning of upgrading the field with new platforms. This modernizing phase will allow the field to produce for another 40 years [2].



Figure 1.1: Location of the Valhall oil field on the NCS [3]

The Valhall field is normally supplied by Power From Shore (PFS) through a High Voltage Direct Current (HVDC) cable from Lista in Southern Norway, which it has since 2013. This transmission line to the Valhall field is 294 km long with a capacity of 78MW. The HVDC cable supplies the field with a more efficient and cleaner supply compared to gas turbines, which is the traditional power generation method for oil and gas platforms. The emissions from Valhall is very low, estimated to be less than 1kg CO_2 per barrel of oil equivalent (boe). To compare, the global average is 15kg CO_2/boe [4].

To this day, the Valhall complex consists of a Wellhead Platform (WP), Injection Platform (IP), Valhall Flank North (VFN), Valhall Flank South (VFS), Valhall Flank West (VFW), Production and Housing (PH) platform, and HOD B, which is an unmanned installation. The field is intended to be upgraded with a Production and Wellhead Platform (PWP), which is connected to the PH platform through a bridge. The field and the platforms are illustrated in Figure 1.2. This implementation of PWP is in a Front-end engineering design (FEED)-phase and will be the basis for this master thesis.

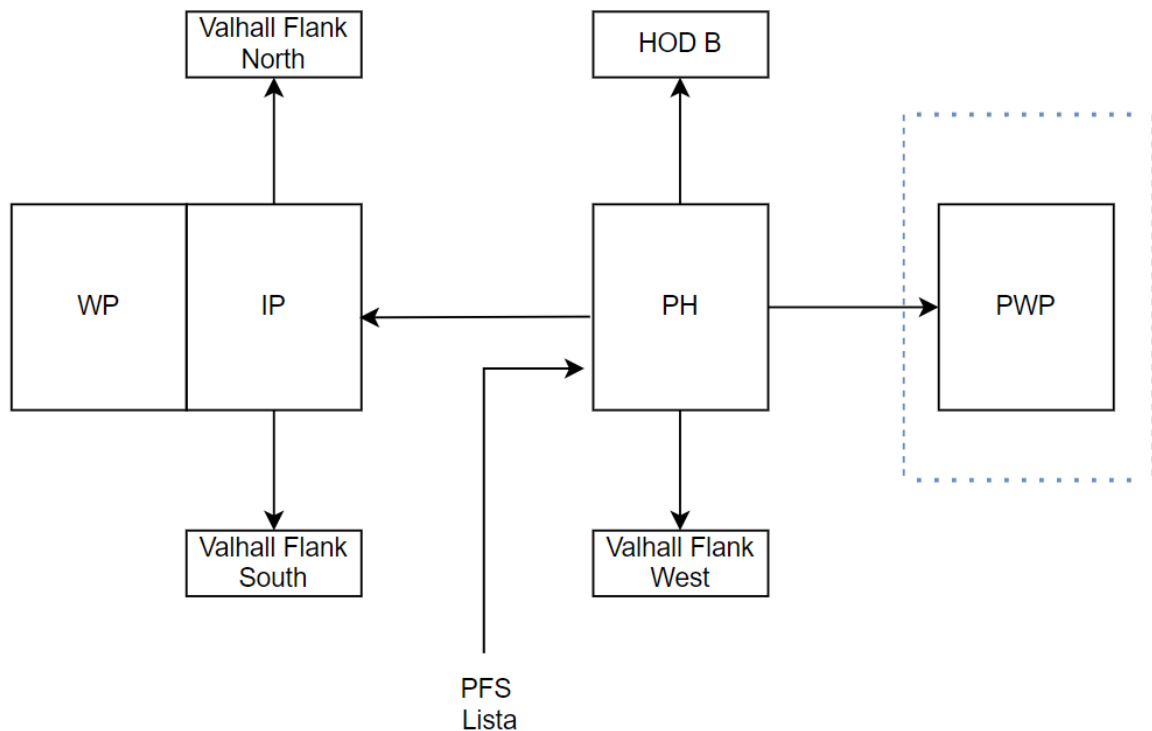


Figure 1.2: Illustration of the Valhall field and the platforms

1.2 Contribution

The modeling of an electrical system of an offshore oil platform that is powered from shore contributes to the field of renewable energy by exploring a practical and feasible solution for meeting energy needs while reducing carbon emissions. This research is particularly significant in the context of Norway's oil production, as Norway is one of the world's largest oil-producing nations, and yet its oil production is comparatively clean compared to other oil nations.

1.3 Objectives

The objective of this thesis is to model and examine the electrical system of the PWP platform at a FEED stage. The focus will be on short-circuit analysis of the platform running under normal operation mode. A case study, considering different combinations of closed and open bus-ties will be conducted to verify that the short-circuit currents are within limits, ensuring the electrical network is modeled to assure safety and reliability.

1.4 Limitations

Due to struggles with the model in DIgSILENT PowerFactory, the scope of work had to be limited quite fairly. Originally, the objective was to do short-circuit calculations for both essential and emergency modes of operation, in addition to normal operation. The goal was also to conduct an arc-flash hazard analysis, but because of the severe time limitations, this had to be opted out. The scope of the work is therefore to do short-circuit analysis under normal operation mode with different combinations of closed and open bus-ties between switchboards.

1.5 Structure

The structure of the thesis is following:

Chapter 2 presents literature review of research done on short-circuit calculations and arc-flash hazard calculations

Chapter 3 explains the theory behind short-circuits and electrical arcs. The focus is mainly on the standards and methods for the calculation of short-circuits and arc-flash. Since IEC 60909 and IEEE 1584 is the method used in the PowerFactory model, these will be the main focus of the theory chapter.

Chapter 4 presents the methodology used for modeling the system in DIgSilent PowerFactory and the calculation settings. It also presents the components of the system. The different cases for the case study is also presented.

Chapter 5 presents and discusses the results from the short-circuit calculations.

Chapter 6 concludes the thesis by summarizing the most important aspects of the analysis results.

Chapter 2

Literature Review

In general, contributions toward the modeling and analysis of offshore oil and gas platforms are limited, but in this chapter research on the analysis of electrical network are considered, as the theory behind the analysis is the same.

The most pertinent literature for the technical aspect related to short-circuit calculations and arc-flash calculations was the books "Power Systems Modelling and Fault Analysis" by Nasser D. Theis [5], "Calculating Short-circuit Currents in Industrial and Commercial Power Systems" published by IEEE [6] and "Arc Flash Hazard Analysis and Mitigation" by J. C. Das [7]. These books were used to obtain knowledge of the theory behind short-circuits and electrical arcs, which will be further addressed in Chapter 3.

In Chapter 3, an investigation of the "IEC 60909-0: Calculation of short-circuit currents in three-phase systems - calculation of currents" [8] and the "IEEE Guide for Performing Arc-Flash Hazard Calculations" [9] will be conducted. These are the main standards intended to utilize when conducting the short-circuit analysis and arc-flash hazard analysis

Some research papers were also explored to inspect how power system analysis has been conducted by others.

Kiing Ing Wong et. al [10] published a research paper titled "Analysis of Electrical Distribution System for Offshore Oil and Gas Platform". The study focused on evaluating the reliability, availability, and maintainability of the distribution system using a simulation-based approach. ETAP was used as a software tool to model the electrical system of a medium-sized offshore oil and gas platform. Load flow analysis and short-circuit analysis were conducted for different operation modes, including normal, service, and emergency operation, as well as a black start case. The short circuit study showed that the worst-case scenario was when all of the three generators were running in parallel. The maximum short-circuit current was utilized to verify if the circuit breaker and fuses have a higher or lower interrupting rating than the maximum short-circuit current. The minimum short-circuit current was also computed and utilized for examining if the relay and fuses were able to trip at the lowest short-circuit currents.

In "Analysis of Load Flow and Short Circuit Studies of an Offshore Platform Using ERACS Software" [11], Hasan, Rao and Mokhtar uses two software (ERCAS and EDSA) to do a load flow and short-circuit analysis of an offshore platform. According to the conducted load flow analysis, there were no voltage violations. For the short-circuit, the results showed that all the loads and equipment are within the defined ratings, except for one bus bar. The circuit current for the respective bus bar must therefore be changed, they concluded.

Zaw and Aung [12] conducted a short-circuit analysis in the software ETAP of a 33/11/0.4kV

distribution system in their paper "Short Circuit Analysis of 33/11/0.4 kV Distribution System Using ETAP". The standard IEC 60909 was used as an approach to conduct the analysis, and for one bus grid, the IEC 613663 was used to describe the current envelope of the transient fault. The short-circuit analysis was conducted for both symmetrical and unsymmetrical faults, for 3-phase, line-to-ground, line-to-line and line-line-ground. In the paper, an overview and methodology of the IEC 60909 are explained along with the necessary formulas.

The paper "Short Circuit Current Algorithm and Software Design Based on IEC60909 Standard" by Huang et al [13] proposed a new and improved algorithm for short-circuit calculations based on IEC 60909. A short-circuit calculation was conducted on a 10-bus system with the new software named FCAP (Fault Current Analysis Software), which is based on an algorithm.

"Arc-Flash Risk Level Calculations based on Computer Simulations and Measures to Avoid Hazards" [14] by Kadir Özen et. al presents an overview over the arc-flash hazard and ways to avoid or reduce hazards. The analysis was conducted in DIgSILENT PowerFactory and is based on the IEEE 1584 and NFPA 70 standards. Important aspects of the theory of arc-flash are presented, like the relationship between incident energy and working distance. The analysis was conducted for different substations with different voltage levels. Different PPE levels and the appropriate equipment for each level were presented. An energy-reducing maintenance switching (ERMS) was also implemented to reduce the arc-flash incident energy.

Along with the update of the IEEE 1584 guide in 2018, Reeves, Freyenberg and Hodder [15] published the "Understanding the Effect of Electrode Configuration on Incident Energy and Arc-Flash Boundary" where the electrode configurations vertical conductors inside metal enclosure (VCB), vertical conductors terminated in insulation barrier inside metal enclosure (VCBB), horizontal conductors inside metal enclosure (HCB) were discussed and analyzed. Usually, for typical working distances, HCB will lead to higher incident energy compared to VCBB and VCB. However, the arc-flash boundary leads to the boundary distance being usually lower for HCB than VCBB and VCB.

Chapter 3

Theory

This chapter consists of the theory behind short-circuits and electrical arcs, which is relevant for being able to do the modeling and analysis.

3.1 Short-Circuit

IEC 60909 defines a short circuit as "accidental or intentional conductive path between two or more conductive parts (e.g. three-phase short circuit) forcing the electric potential differences between these conductive parts to be equal or close to zero" (IEC, 2016, s. 8). Short-circuit calculations are a major part of electric power system analysis, planning, and operation. Power systems and industrial systems are carefully engineered to ensure the safe and reliable supply of loads. One crucial aspect considered during the design and operation of electrical systems is the effective management of short-circuits. While every effort is made to prevent short-circuits, they can still occur. When a short-circuit happens, it often leads to the flow of large and uncontrollable currents. Failure to promptly detect and address this condition can result in damage to equipment, widespread disruptions beyond the faulted section, and pose risks to personnel. Hence, a well-designed system aims to isolate short-circuits safely, minimizing equipment damage and system downtime.[6] The occurrence of faults can be attributed to several factors, including:

- Overheating caused by loose connections.
- Voltage surges, where there is a sudden rise of voltage that can damage the equipment.
- Deterioration of equipment over time.
- Excessive voltage or mechanical stresses to the equipment, surpassing its design limits and causing breakdowns.
- Assembly of moisture and contaminants, which can impair the equipment's performance.
- Contact with a metallic or conducting object, e.g. tools.
- Operation of the system in an inappropriate manner.

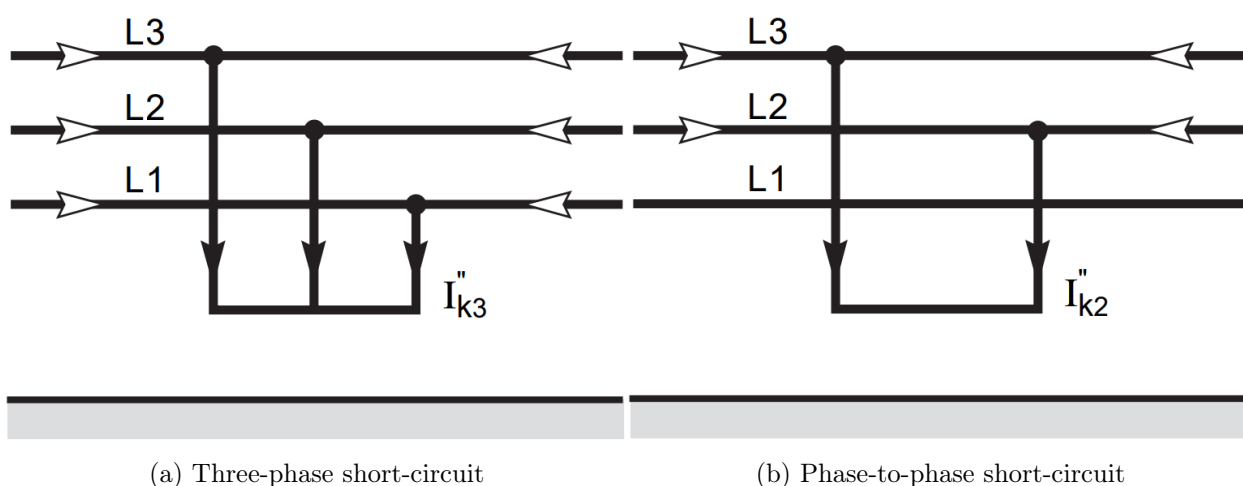
Short-circuit calculations are necessary both during the planning phase of the electrical system, as well as while the network is in use operation mode. Some typical practices where short-circuit analysis and calculations are conducted are listed below [16].

- **Equipment Short-Circuit Capacity:** One important application is ensuring that the short-circuit capacity of the equipment is not exceeded during system expansion or strengthening. By analyzing the potential short-circuit currents, engineers can determine if the existing equipment can handle the increased fault levels or if upgrades are necessary.

- **Protective Equipment Coordination:** Short-circuit analysis is also essential for coordinating protective equipment such as fuses, over-current relays, and distance relays. By understanding the expected fault currents, it is possible to set the appropriate settings and coordination curves to ensure selective and effective protection.
- **Earth Grounding System Design:** Dimensioning earth grounding systems is another application of short-circuit analysis. By evaluating the fault currents and system parameters, engineers can determine the required size and configuration of the grounding system to ensure safe operation and effective fault current dissipation.
- **Cable and Transmission Line Thermal Limits:** Another application is the verification of the permitted thermal limits of cables and transmission lines. By calculating the short-circuit currents and considering the cable or line specifications, engineers can determine if the fault currents pose a risk of overheating or damaging the equipment, and this can be useful when selecting cables and their size.

A fault in a power system refers to an uncommon state where there is an electrical malfunction in the equipment operating at the primary voltages of the system. Typically, there are two main types of failures that can arise. The first type is an insulation failure, which leads to a short-circuit fault. This type of fault can happen due to various reasons, such as prolonged stress and degradation of the insulation over time or a sudden surge in voltage. Another type of fault is when there is a disruption of current flow, known as an open-circuit fault. This can happen when there is a break or interruption in the electrical path. [5]

In a short-circuit analysis, it is interesting to examine both the maximum and the minimum short-circuit current. The maximum short-circuit currents are used to determine the capacity and rating of the electrical equipment, whereas the minimum short-circuit current which can be the basis for the selection of fuses for protective devices or for checking the run-up of motors. Short-circuit faults can happen between different phases and earth. The different types of short-circuit faults are illustrated in Figure 3.2. Phase-to-earth is the most common fault and stands for approximately 80% of faults. Phase-to-phase represents 15% of faults, while three-phase only represents 5% of the faults. [17]



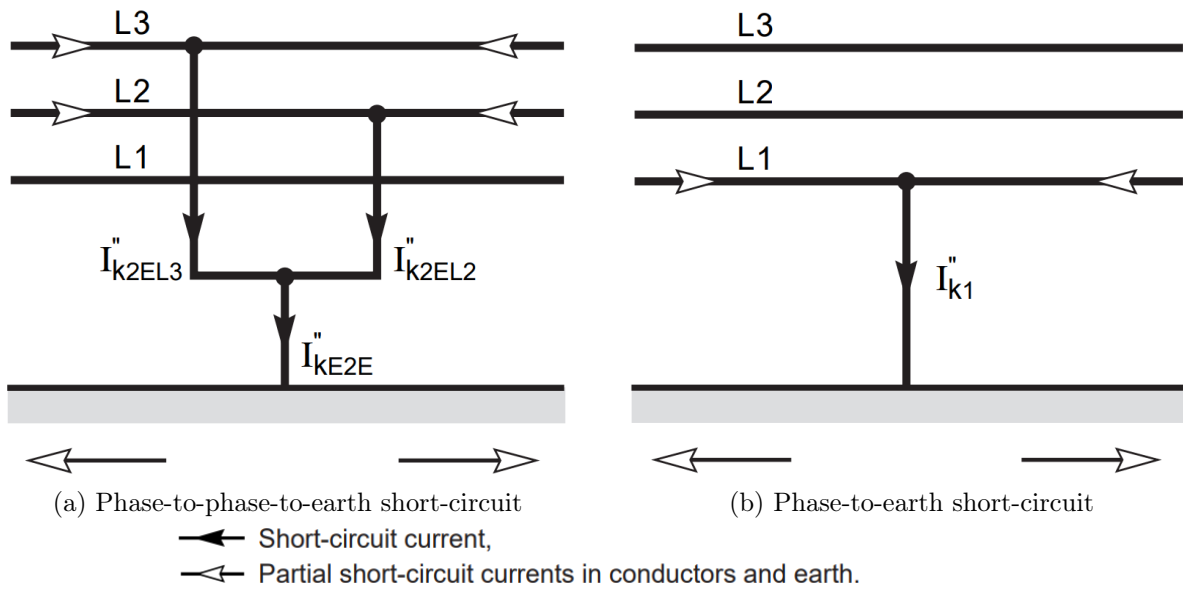


Figure 3.2: Short-circuit types according to IEC 60909 [8] [17]

3.1.1 Standards

Different methods and standards are applied to obtain adequate values without having to have detailed network information. Some of the most utilized methods are listed below. [18]

- IEC 60909 method is in low- and high-voltage three-phase AC systems and is an international standard.
- ANSI method is used for short-circuit calculations of Alternating current (AC)-systems in Northern America and is based on the IEEE C37.010 standard.
- Complete method is based on the superposition method and is often used for existing networks that are under operation.
- IEC 61363 method is used for marine or offshore systems, e.g boats and ships.
- IEC 61660 (DC) method is the International Electrotechnical Commission (IEC) standard for short-circuit currents in Direct current (DC)-systems.
- ANSI/IEEE 946 (DC) method is the ANSI/IEEE for DC-systems.

Figure 3.3 shows a comparison of two methods for calculating short-circuits. The IEC 60909 is a simplified method based on a standard, whereas the complete method is not based on a standard but a extensive set of data, which in theory will make the complete method more accurate.

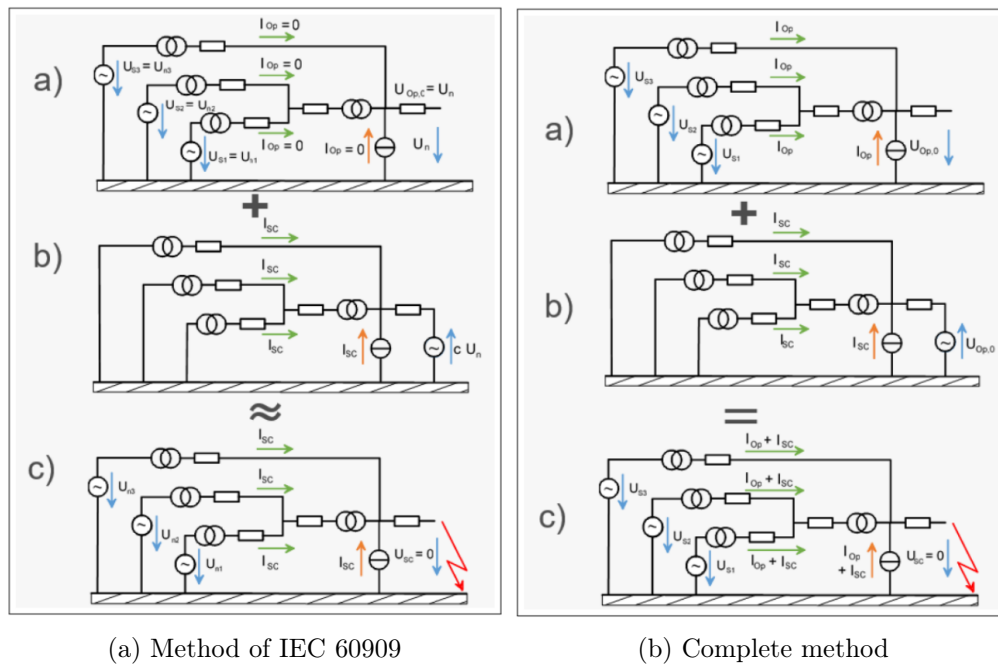


Figure 3.3: Comparison of two methods for short-circuit calculations [16]

IEC 60909 is the method that will be used in this master's thesis, and will therefore be examined in more depth. The following formulas used in this section are based on IEC 60909 [8].

3.1.2 IEC 60909

IEC 60909 is a short-circuit calculation standard carried out by the IEC for power systems with voltage levels under 500kV. Using this method, engineers can compromise accuracy and calculation simplicity while providing safe results. [19]. IEC 60909 method is based on using an equivalent voltage source at the location where the short-circuit fault occurs. In the event of a short-circuit fault, a virtual equivalent voltage source is inserted at the location of the fault, becoming the sole voltage source in the network. The other power sources are disregarded, and instead, their internal impedance is taken into account [19]. Figure 3.4 shows an equivalent circuit diagram where a transformer is connected.

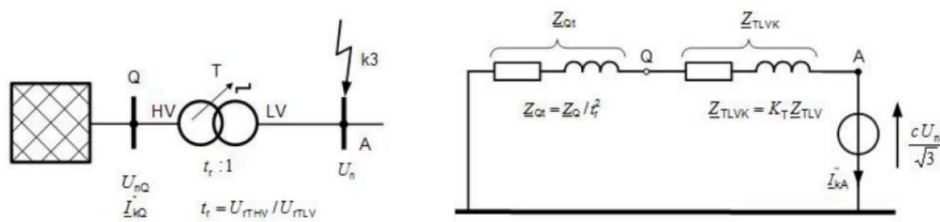


Figure 3.4: Equivalent circuit diagram for a network with transformer [8]

According to IEC60909, a complete short-circuit calculation, the current at the fault location should be expressed as a function of time [8]. Figure 3.5 shows the short circuit current as a time function with a decaying AC component. After the occurrence of a short circuit fault, it is interesting to examine values such as the initial symmetrical short circuit current, I_k'' , the steady-state short circuit current, I_k , the peak short circuit current i_p and the short circuit's DC-component, i_{DC} which is the aperiodic component of the instantaneous current.

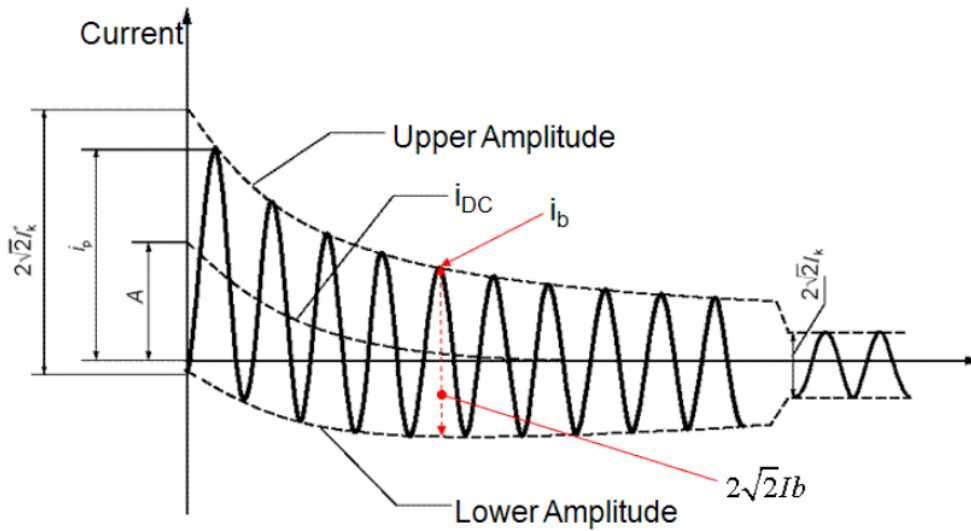


Figure 3.5: Short-circuit current as a function of time with decaying AC component [16]

IEC 60909 uses a safety factor, Safety factor (c-factor), which is a voltage correction factor that ensures that the estimations and short-circuit calculations are adequate results.

Table 3.1: Voltage factor, c, for calculating the minimum and maximum short-circuit currents

Nominal voltage of system U_n [V]	Tolerance	Voltage factor	
		c_{min}	c_{max}
100 - 1000	$\pm 6 \%$	0.95	1.05
	$\pm 10 \%$	0.95	1.10
$>1\ 000$	-	1.00	1.10

3.1.3 Impedances, Z

When there is a fault between two points in an equivalent circuit, the impedance between these points is insignificant, which leads to a significantly high short-circuit current. The short circuit current is determined by the impedance Z , which depends on the reactance X and resistance R . Equation 3.1 describes the short-circuit impedance.

$$Z = \sqrt{R^2 + X^2} \quad (3.1)$$

Equation 3.2 to 3.4 describes the impedances based on reactance and resistance, for two-winding transformers.

$$Z_T = \frac{u_{kr}}{100\%} \times \frac{U_{rT}^2}{S_{rT}} \quad (3.2)$$

$$R_T = \frac{u_{Rr}}{100\%} \times \frac{U_{rT}^2}{S_{rT}} = \frac{P_{krT}}{3 \times I_{rT}^2} \quad (3.3)$$

$$X_T = \sqrt{Z_T^2 - R_T^2} \quad (3.4)$$

Where, U_{rT} is the transformer-rated voltage, I_{rT} is the rated current of the transformer and S_{rT} is the transformer-rated apparent power. P_{krT} is the loss in the transformer windings, u_{kr} is the rated short-circuit voltage and u_{Rr} is the rated resistive component of u_{kr} .

3.1.4 Initial Symmetrical Short-Circuit Current, I_k''

The initial symmetrical short-circuit current, I_k'' is the rms value of the short-circuit's AC component, and have different formulas based on the type of short-circuit. See Figure 3.2 for the different types. The Equations for I_k'' for three-phase, phase-to-phase, phase-to-phase-to-earth and phase-to-earth short circuit are shown in Equation 3.5 to 3.11, respectively.

Three-phase short-circuit

$$I_{k3}'' = \frac{c \times U_n}{\sqrt{3} \times Z_k} = \frac{c \times U_n}{\sqrt{3} \times \sqrt{R_k^2 + X_k^2}} \quad (3.5)$$

Phase-to-phase short-circuit

$$I_{k2}'' = \frac{\sqrt{3}}{|Z_1 + Z_2|} \times \frac{c \times U_n}{\sqrt{3}} \quad (3.6)$$

If the impedances, Z_1 and Z_2 , is equal, the phase-to-phase initial symmetrical short circuit current can be expressed as Equation 3.7

$$I_{k2}'' = \frac{c \times U_n}{|2Z_k|} = \frac{\sqrt{3}}{2} I_{k3}'' \quad (3.7)$$

Phase-to-phase-to-earth short-circuit

$$I_{k2EL2}'' = \left| \frac{\sqrt{3}(Z_0 - aZ_2)}{Z_1Z_2 + Z_1Z_0 + Z_2Z_0} \right| \times \frac{c \times U_n}{\sqrt{3}} \quad (3.8)$$

$$I_{k2EL3}'' = \left| \frac{\sqrt{3}(Z_0 - a^2Z_2)}{Z_1Z_2 + Z_1Z_0 + Z_2Z_0} \right| \times \frac{c \times U_n}{\sqrt{3}} \quad (3.9)$$

$$I_{kE2E}'' = \left| \frac{3Z_2}{Z_1Z_2 + Z_1Z_0 + Z_2Z_0} \right| \times \frac{c \times U_n}{\sqrt{3}} \quad (3.10)$$

Phase-to-earth short-circuit

$$I_{k1}'' = \frac{3}{|Z_1 + Z_2 + Z_0|} \times \frac{c \times U_n}{\sqrt{3}} \quad (3.11)$$

3.1.5 Peak Short-Circuit Current, i_p

The peak short-circuit current, i_p , is the largest possible instantaneous value of the short-circuit current, and can be derived from Equation 3.12.

$$i_p = \kappa \sqrt{2} I_k'' \quad (3.12)$$

Where the coefficient κ can be derived from Equation 3.13 and is dependent on R/X-ratio.

$$\kappa = 1.02 + 0.98 \times e^{\frac{-3R}{x}} \quad (3.13)$$

Figure 3.6 illustrates the relation between the coefficient κ and the R/X- ratio and X/R-ratio, respectively.

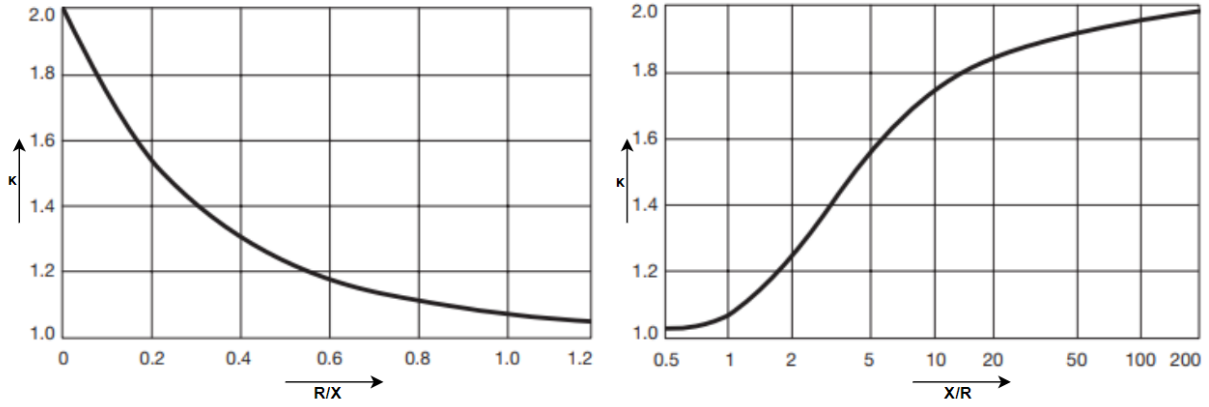


Figure 3.6: The value κ to the R/X- or X/R-ratio [8]

The X/R-ratio, and thence the coefficient κ , is calculated in accordance with either method A, B, or C:

- **Method A:** Uniform R/X- or X/R-ratio
Uses the smallest R/X-ratio or the largest X/R-ratio for all the contributing branches.
- **Method B:** R/X- or X/R-ratio at the fault location
The coefficient is increased with $\kappa = \kappa \times 1.15$ to eliminate inaccuracies caused by R/X-or X/R-ratio because of complex impedances in the network.
- **Method C:** Equivalent frequency, f_c
For meshed systems, C is the recommended method. Z_C , an equivalent impedance ($Z_C = R_C + jX_C$) is calculated as seen from the fault location, see Equation 3.14 For nominal frequency $f = 50Hz$, the assumed frequency $f_C = 20Hz$, and for $f = 60Hz$, it is $f_C = 24Hz$.

$$\frac{R}{X} = \frac{R_C}{X_C} \times \frac{f_c}{f}, \quad \frac{X}{R} = \frac{X_C}{R_C} \times \frac{f}{f_c} \quad (3.14)$$

3.1.6 Symmetrical Short-Circuit Breaking Current, I_b

When the short-circuit fault occurs far from the generator, the symmetrical short-circuit breaking current, I_b will be equal to the initial symmetrical short-circuit I_k'' and the steady-state short-circuit current I_k .

$$I_b = I_k'' = I_k \quad (3.15)$$

For short-circuits that occur near the generator, Equation 3.16 and 3.17 can be used to calculate the symmetrical short-circuit breaking current for synchronous and asynchronous machines, respectively. This I_b value is used to determine the breaking capacity of circuit breakers.

$$I_b = \mu I_k'' \quad (3.16)$$

$$I_b = \mu q I_k'' \quad (3.17)$$

The coefficients, μ and q are ac-decay-related factors. μ is defined by minimum time delay (t_{min}) and the ratio between the initial short-circuit current and the rated current of the generator (I_k''/I_r). q is also dependent on the minimum time delay (t_{min}), as well as the active power of the machine. See Figure 3.7 for factor μ and q .

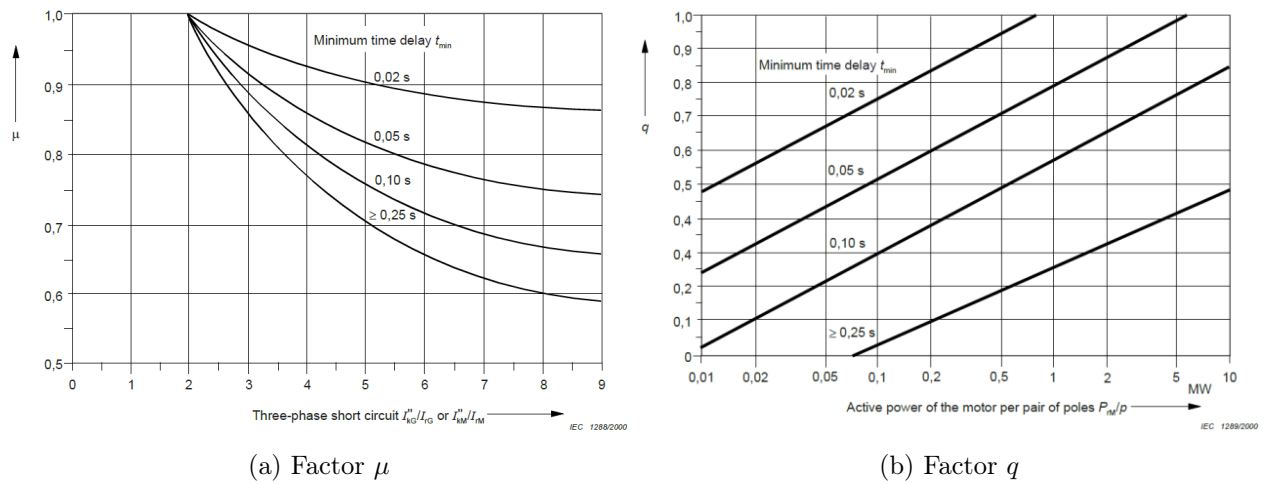


Figure 3.7: Graphs for determining μ and q for calculation of I_b [8]

3.1.7 DC-Component of the Short-Circuit Current, i_{DC}

The decaying aperiodic component of the short-circuit current can be derived from Equation 3.18.

$$i_{DC} = \sqrt{2}I_k'' e^{-2\pi ftR/X} \quad (3.18)$$

3.1.8 Steady-State Short-Circuit Current, I_k

The steady-state short-circuit current, I_k , is affected by the saturation of the generator, thus the calculation for I_k is less accurate than for I_k'' [17]. Equation 3.19 and 3.20 are adequately precise for the calculation of maximum- and minimum steady-state short-circuit currents. I_r is the generator's rated current and the factor λ is dependent on the saturated synchronous reactance of a generator.

$$I_{kmax} = \lambda_{max} I_r \quad (3.19)$$

$$I_{kmin} = \lambda_{min} I_r \quad (3.20)$$

3.2 Electrical Arc

An electrical arc is an electrical discharge that occurs between two conductors through a gas, such as air, resulting in the generation of bright light, heat, and often noise. The characteristics of an electrical arc are influenced by various factors, including the size of the gap between two electrodes, the composition of the terminal material, the voltage across the arc, and the conductivity of the surrounding medium [9]. An arc can happen in both DC circuits and AC circuits. If the arc occurs in an AC circuit, it can re-occur on every half-circuit of the current [20].

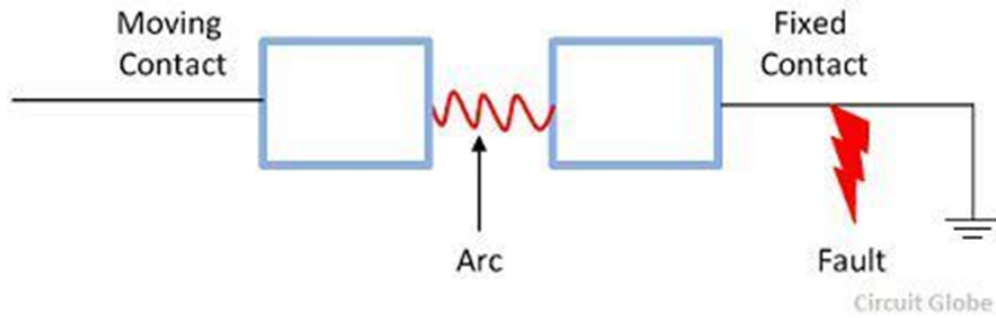


Figure 3.8: The principle behind an electrical arc [20]

3.2.1 Arcing in Cubicle

The formation of an electrical arc inside a cubicle can be represented by steps A to D illustrated in Figure 3.9, where the buildup of pressure over time is shown. Section A represents the compression phase where the pressure builds up and B is the expansion phase where it happens a relief of the built-up pressure. Section C represents the emission stage, where the air is emitted and the pressure is steadying. D represents the thermal phase, which endures until the arc is extinguished [7].

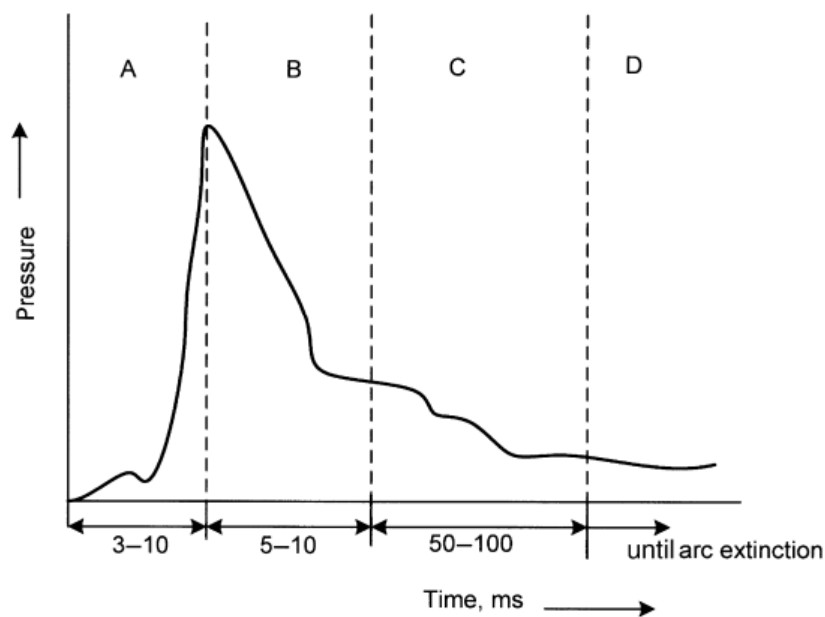


Figure 3.9: The stages of arc formation in a cubicle [7]

3.2.2 Arc Flash

The standard IEEE 1584 [9] describes arc flash as "a dangerous condition associated with the release of energy by an electric arc" and can lead to hazards like thermal burns, intense light and sound, fire, pressure waves, and toxic gases [7]. Operating an electrical facility can pose significant hazards, with arc flash being one of the main risks. If the operator does not have access to the appropriate Personal Protective Equipment (PPE) and if the protective relays are not properly designed, they can be exposed to severe, and potentially fatal, injuries. [21]

3.2.3 IEEE 1584

IEEE 1584 is a guide for performing arc-flash hazard calculations and supplies a step-by-step method for computing the incident thermal energy and the arc-flash boundary. The guide applies to three-phase ac-systems with voltages ranging from 208V to 15kV [9]. In this section, the steps from the IEEE 1584 guide will be addressed.

Step 1: Collect system and installation data

The first step in the process of conducting an arc flash analysis is to collect system and installation data and is a time-consuming part of the process. The required data for conducting an arc flash analysis is similar as for short-circuit analysis. In this step, typical information that should be collected is information about equipment like switchgear, motor-starters, switchboards, switches and circuit breakers, control panels, sockets, etc. After the collection of information, a short-circuit analysis should be done and obtain necessary information such as fault current, X/R ratio, nameplate data, and conductor/cable data [9]

Step 2: Determine operation modes of the system

Step number two is to determine the different operation modes of the system. Examples of different modes of operation can be:

- Normal operation
- Essential operation
- Emergency operation

Under the different operation modes, different scenarios can be conducted. For instance, bus-ties open or closed, activation of one or more utility feeders, shutdown or startup.

Step 3: Determine the bolted fault currents in the system

The fault currents are retrieved from the short-circuit calculations and analysis. It is essential to consider both higher and lower available short-circuit currents as they can lead to varying levels of available arc-flash energies. Higher fault currents tend to result in shorter trip times for overcurrent protective devices. This short trip time can lead to the incident energy being lower. High short-circuit currents without reducing opening time can result in higher incident energy. On the other hand, lower short-circuit currents can result in longer opening times, and thus a higher incident energy.

Step 4: Determine Bus Gap and Enclosure Size for Different System Voltages and Equipment Class

Step number four is to assess each equipment component included in the study, and determine the typical gaps between conductors based on the system voltage and the equipment class. Table 3.2 shows the different typical bus gaps for each equipment class and its respective typical enclosure size. This enclosure size is used to find the correction factor for the enclosure size incident energy.

Table 3.2: Typical bus gaps and enclosure size for different equipment classes [9]

Equipment class	Bus gap	Enclosure Size (HxWxD)
15 kV switchgear	152 mm	1143 mm × 762 mm × 762 mm
15 kV MCC	152 mm	914.4 mm × 914.4 mm × 914.4 mm
5 kV switchgear	104 mm	914.4 mm × 914.4 mm × 914.4 mm
5 kV switchgear	104 mm	1143 mm × 762 mm × 762 mm
5 kV MCC	104 mm	660.4 mm × 660.4 mm × 660.4 mm
Low-voltage switchgear	32 mm	508 mm × 508 mm × 508 mm
Shallow low-voltage MCCs and panelboards	25 mm	355.6 mm × 304.8 mm × >203.2 mm
Deep low-voltage MCCs and panelboards	25 mm	355.6 mm × 304.8 mm × >203.2 mm
Cable junction box	13 mm	355.6 mm × 304.8 mm × >203.2 mm

Step 5: Determine Electrode Configuration of the Equipment

The electrode configuration affects the incident energy and the arc flash boundary. Electrodes can be installed in open-air (OA) or enclosed inside a metal box (B), and can be either vertically (V) or horizontally (H) oriented. It can also be barrier-terminated (B). There are five different electrode configurations listed in IEEE 1584; vertical electrodes in metal box enclosure (VCB), Vertical electrodes barrier terminated inside metal box enclosure (VCBB), horizontal electrodes in metal box enclosure (HCB), open-air vertical electrodes (VOA) and open-air horizontal electrodes (HOA). [22]

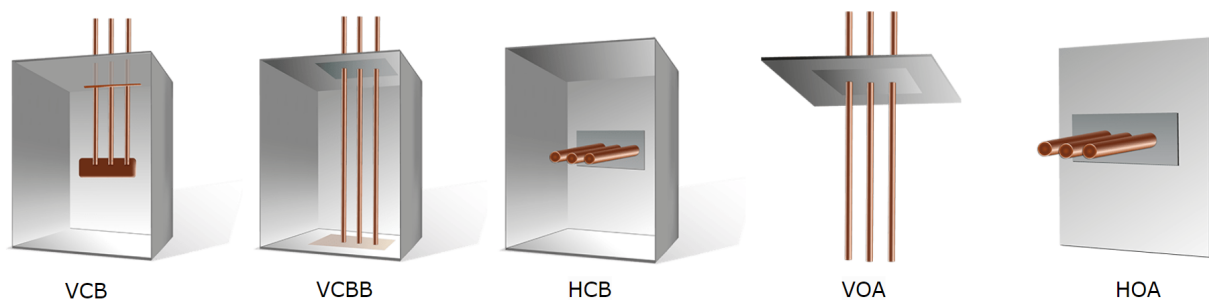


Figure 3.10: Electrode configurations [23]

Step 6: Determine Working Distances

Table 3.3 shows the typical working distance for personnel used for calculating the incident energy.

Table 3.3: Typical working distance different equipment classes

Equipment class	Working distance
15 kV switchgear	914.4 mm
15 kV MCC	914.4 mm
5 kV switchgear	914.4 mm
5 kV switchgear	914.4 mm
5 kV MCC	914.4 mm
Low-voltage switchgear	609.6 mm
Shallow low-voltage MCCs and panelboards	457.2 mm
Deep low-voltage MCCs and panelboards	457.2 mm
Cable junction box	457.2 mm

Step 7: Calculate the Arcing Current

To obtain the arcing current, Equation 3.21 is utilized. The equation is valid for V_{oc} 600V, 2700V, 14300V.

$$I_{arcV_{oc}} = 10^{(k1+k2lgI_{bf}+k3I_gG)} (k4I_{bf}^6 + k5I_{bf}^5 + k6I_{bf}^4 + k7I_{bf}^3 + k8I_{bf}^2 + k9I_{bf} + k10) \quad (3.21)$$

Where, $I_{arcV_{oc}}$ is the average arcing current at an open-circuit voltage, V_{OC} . G is the gap between the electrodes, and $k1$ to $k10$ are coefficients based on the system voltage and electrode configuration. The coefficients are attached in Appendix A.1.

Step 8: Determine the Duration of the Arc

The duration of the arc is the time it takes before the source of energy stops supplying energy to the arc fault or how long time it takes the protective device to stop the arc current. Usually, it is possible to find the tripping time and clearing time in the manufacturer's time-current curve for fuses and circuit breakers.

Step 9: Calculate Incident Energy

To obtain the incident energy, Equation 3.22 is utilized. The equation is valid for V_{oc} 600V, 2700V, 14300V.

$$E_{V_{oc}} = \frac{12.552}{50} T \times 10^{(k1+k2lgG + \frac{k3I_{arc,V_{oc}}}{k5I_{bf}^6 + k6I_{bf}^5 + k7I_{bf}^4 + k8I_{bf}^3 + k9I_{bf}^2 + k10I_{bf}}) + k11lgI_{bf} + k12lgD + k13lgI_{arc,V_{oc}} + lg(\frac{1}{CF})} \quad (3.22)$$

Where $E_{V_{oc}}$ is the incident energy at v_{oc} , T is the duration of the arc in ms, G is the conductor gap, $I_{arcV_{oc}}$ is the arcing current, D is the working distance in mm, CF is the correction factor and $k1$ to $k13$ are coefficients based on the system voltage and electrode configuration. The coefficients are attached in Appendix A.2

Step 10: Determine Arc-Flash Boundary

To determine the arc-flash boundary, AFB, Equation 3.23 is utilized. The distance from the arc where the incident energy is $1.2cal/cm^2$ is the AFB. The equation is valid for V_{oc} 600V, 2700V, 14300V.

$$AFB_{V_{oc}} = 10^{\frac{k1+k2lgG + \frac{k3I_{arc,V_{oc}}}{k4I_{bf}^7 + k5I_{bf}^6 + k6I_{bf}^5 + k7I_{bf}^4 + k8I_{bf}^3 + k9I_{bf}^2 + k10I_{bf}} + k11lgI_{bf} + k13lgI_{arc,V_{oc}} + lg(\frac{1}{CF}) - lg(\frac{20}{T})}{-k12}} \quad (3.23)$$

Where $AFB_{V_{oc}}$ is the arc-flash boundary at v_{oc} , T is the duration of the arc in ms, G is the conductor gap, $I_{arcV_{oc}}$ is the arcing current, D is the working distance in mm, CF is the

correction factor and k_1 to k_{13} are coefficients based on the system voltage and electrode configuration. The coefficients are attached in Appendix A.2

3.2.4 PPE

While IEEE 1584 does not provide specific categories of protective clothing, NFPA 70E has guidance on the selection and use of Personal Protective Equipment (PPE) for arc flash hazards. Figure 3.11 shows the recommended protective clothing that should be worn at energy levels where there is a risk of exposure to arc flash hazards. [24]





Hazard/Risk Category 4 cal/cm ² 1	Arc-rated long-sleeve shirt Arc-rated pants or overall Arc-rated face shield with hard hat Safety glasses Hearing protection Leather & voltage rated gloves (as needed) Leather work shoes	
Hazard/Risk Category 8 cal/cm ² 2	Arc-rated long-sleeve shirt Arc-rated pants or overall Arc-rated face shield & balaclava or Arc flash suit with hard hat Safety glasses, Hearing protection Leather & voltage rated gloves (as needed) Leather work shoes	
Hazard/Risk Category 25 cal/cm ² 3	Arc-rated long-sleeve jacket Arc-rated pants Arc-rated flash hood with hard hat Safety glasses, Hearing protection Leather & voltage rated gloves (as needed) Leather work shoes	
Hazard/Risk Category 40 cal/cm ² 4	Arc-rated long-sleeve jacket Arc-rated pants Arc-rated flash hood with hard hat Safety glasses, Hearing protection Leather & voltage rated gloves (as needed) Leather work shoes	

Figure 3.11: Protective Clothing according to NFPA 70E [14]

Chapter 4

Methods

This chapter presents the methodology for the modeling and analysis conducted in this thesis.

4.1 Collection of Data

In this master’s thesis, data collection was a significant part of the task at hand. To simulate the electrical model accurately, a vast amount of data was required. Aker Solutions provided various documents like electrical Load List [25], high voltage transformer data sheet [26] [27], high voltage switchgear data sheet [28] and low voltage switchgear data sheet [29]. Cable catalogs and preliminary cable sizes were also provided. As the project development is in a FEED phase, which means that things were not yet completely finalized, many values had to be adjusted and modified along the way.

4.2 Modeling in DIgSILENT PowerFactory

The electrical model of PWP was modeled in DIgSILENT PowerFactory and is displayed in Figure 4.1. The system consists of 14 bus bars, which are listed in Table 4.1. The network consists of a high voltage power system, where the nominal voltage $U_n > 1000V$, and a low voltage power system where $U_n < 1000V$. The design principles are according to Aker BP’s power system philosophy [30].

Table 4.1: Different switchboards located on the platform

Tag	Voltage U_n	Description
60-EH-19000A	11 <i>kV</i>	Switchboard A
60-EH-19000B	11 <i>kV</i>	Switchboard B
60-EH-19001	20 <i>kV</i>	Fenris UI Umbilical Supply Switchboard
60-EN-19020A	690 <i>V</i>	Utility Switchboard A
60-EN-19020B	690 <i>V</i>	Utility Switchboard B
60-EN-19010A	690 <i>V</i>	Process Switchboard A
60-EN-19010B	690 <i>V</i>	Process Switchboard B
60-EN-19013	690 <i>V</i>	Emergency Switchboard
60-EL-19011A	400/230 <i>V</i>	Process Main Distribution Board A
60-EL-19011B	400/230 <i>V</i>	Process Main Distribution Board B
60-EL-19021A	400/230 <i>V</i>	Utility Main Distribution Board A
60-EL-19021B	400/230 <i>V</i>	Utility Main Distribution Board B
60-EL-19013A	400/230 <i>V</i>	Emergency Main Distribution Board
60-EL-19008	440 <i>V</i>	Well Intervention Switchboard

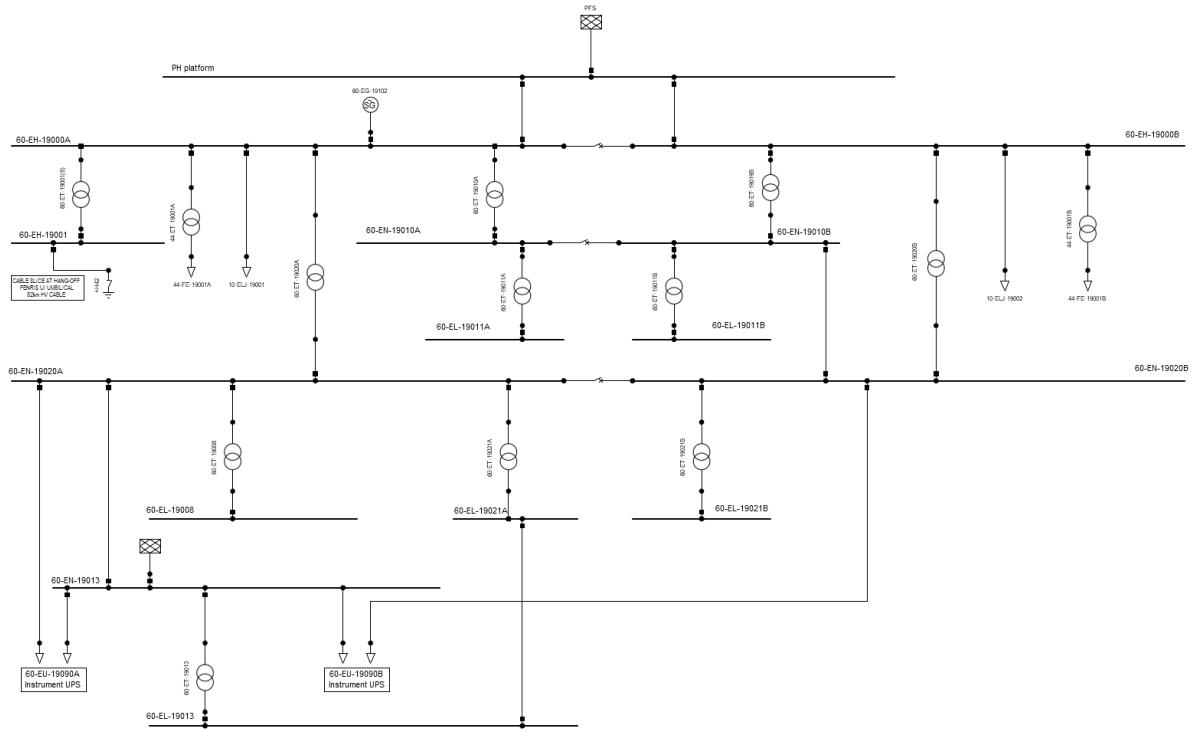


Figure 4.1: Electrical model

4.2.1 High Voltage System

The High Voltage (HV) power system consists of two 11kV switchboards (60-EH-19000A/B) and a 20kV switchboard (60-EH-19001). The 11kV switchboards are supplied from the PH platform, which is powered from shore. The 20kV switchboard is fed by 60-EH-19000A through an 11/20kV transformer. From the 20kV switchboard, PWP will be fed further to Fenris Unmanned Installation (UI) located 50km away, through equipment and pipelines on the seabed.

The HV power system's main components are four 11/0.69kV transformers to the utility and process switchboard, two 11/6.6kV transformers to the Medium Heaters (44-FE-19001A/B), an 11/20kV transformer to the 20kV switchboard, as well as 11kV and 20kV HV switchgear. The drilling rig interfaces (10-ELJ-19001/2) are modeled as 8MW load, whereas the Medium Heaters (44-FE-19001A/B) are modeled as 3.8MW loads. The HV transformers are listed in Table 4.2.

Table 4.2: HV transformer data

Transformer tag	U_{rT} [kV]		S_{rT} [MVA]		u_{kr} [%]		X/R-ratio	Winding
	Prim	Sec	AN	AF	AN	AF		
60-ET-19001	11	20	2.5	-	7	-	8	Dyn11
44-ET-19001A	11	6.6	4	4.4	7	7.7	8	Dyn11
44-ET-19001B	11	6.6	4	4.4	7	7.7	8	Dyn11
60-ET-19020A	11	0.69	3.15	4.2	7	9.3	8	Dyn11
60-ET-19020B	11	0.69	3.15	4.2	7	9.3	8	Dyn11
60-ET-19010A	11	0.69	3.15	4.2	7	9.3	8	Dyn11
60-ET-19010B	11	0.69	3.15	4.2	7	9.3	8	Dyn11

Some assumptions were made in regard to the transformers. The zero sequence impedance, z_0 , is assumed to be the same as the positive sequence impedance, z_1 . In DIGSILENT PowerFactory, the positive sequence impedance is based on the short-circuit voltage u_{kr} and the

X/R-ratio. The values for X/R-ratio are assumed based on typical short-circuit losses for a 3.15/4.20MVA transformer, where a value of 8 for the X/R-ratio was seen as a good fit. [31] The rated short circuit voltage u_{kr} is often given only for the Air Natural (AN)-rating for the transformer. To obtain the AF-rated short-circuit voltage, Equation 4.1 was utilized.

$$u_{Kr(AF)} = u_{Kr(AN)} \times \frac{S_{rT(AF)}}{S_{rT(AN)}} \quad (4.1)$$

The HV system is also equipped with an essential generator (60-EG-19102) which is an 11kV, 3.75MVA diesel-driven generator. The essential generator will be able to assist the PWP electrical system under an essential operating mode, and will then be run in parallel with essential generators on the PH platform.

HV Cables

Two different types of cables are used for the HV cables: Draka FlexFlame RFOU 6/10(12)kV P3/P10 Power cable [32] and Draka FlexFlame RFOU 12/20(24)kV Power cable [33]. The HV cables with their respective size, length, and number of parallel lines are listed in Table 4.3.

Table 4.3: High Voltage Main Cables

FROM	TO	L [m]	TYPE	SIZE	Parallels
60-EH-9000A	60-EH-19000A	328	RFOU 6/10(12)kV, P3/P10	1c x 300mm ²	3
60-EH-9000B	60-EH-19000B	328	RFOU 6/10(12)kV, P3/P10	1c x 300mm ²	3
60-EG-19012	60-EH-19000A	100	RFOU 6/10(12)kV, P3/P10	1c x 185mm ²	1
60-EH-19000A	60-ET-19001	60	RFOU 6/10(12)kV, P3/P10	1c x 185mm ²	1
60-ET-19001	60-EH-19001	60	RFOU 12/20(24)kV, P19/P21	1c x 95mm ²	1
60-EH-19001	UI Cable Splice	100	RFOU 12/20(24)kV, P19/P21	1c x 95mm ²	1
60-EH-19000A	44-ET-19001A	60	RFOU 6/10(12)kV, P3/P10	1c x 95mm ²	1
60-EH-19000B	44-ET-19001B	60	RFOU 6/10(12)kV, P3/P11	1c x 95mm ²	1
60-EH-19000A	10-ELJ-19001	150	RFOU 6/10(12)kV, P3/P10	1c x 300mm ²	1
60-EH-19000B	10-ELJ-19002	150	RFOU 6/10(12)kV, P3/P10	1c x 300mm ²	1
60-EH-19000A	60-ET-19020A	50	RFOU 6/10(12)kV, P3/P10	1c x 185mm ²	1
60-EH-19000B	60-ET-19020B	50	RFOU 6/10(12)kV, P3/P10	1c x 185mm ²	1
60-EH-19000A	60-ET-19010A	50	RFOU 6/10(12)kV, P3/P10	1c x 185mm ²	1
60-EH-19000B	60-ET-19010B	50	RFOU 6/10(12)kV, P3/P10	1c x 185mm ²	1

4.2.2 Low Voltage System

The Low Voltage (LV) power system consists of eleven different switchboards and distribution boards with different levels of voltage (690V, 440V, and 400/230V). The distribution boards are used to feed the smaller power consumers, including socket outlets, heat tracing, and lightning. These LV bus bars are separated into four different types:

- Utility
- Process
- Emergency
- Well Intervention

The same assumptions were done for the LV transformers as for the HV transformers. An X/R ratio of 5 was assumed for the 690/400V transformers. The LV transformers are listed in Table 4.4.

Table 4.4: LV transformer data

Transformer tag	U_{rT} [kV]		S_{rT} [MVA]		u_{kr} [%]		X/R-ratio	Winding
	Prim	Sec	AN	AF	AN	AF		
60-ET-19011A	0.69	0.4	0.5	-	7	-	5	Dyn11
60-ET-19011B	0.69	0.4	0.5	-	7	-	5	Dyn11
60-ET-19021A	0.69	0.4	0.5	-	7	-	5	Dyn11
60-ET-19021B	0.69	0.4	0.5	-	7	-	5	Dyn11
60-ET-19013A	0.69	0.4	0.25	-	4	-	5	Dyn11
60-ET-19008	0.69	0.44	0.5	-	6	-	5	Dyn11

LV Cables

Draka FlexFlame BFOU 0.6/1(1.2)kV P5/P12 Power cable was used for the LV cables [34]. The LV cables with their respective size, length, and number of parallel lines are listed in Table 4.5.

Table 4.5: Low Voltage Main Cables

FROM	TO	L (m)	TYPE	SIZE	Parallels
60-ET-19020A	60-EN-19020A	50	BFOU 0.6/1(1.2)kV P5/P12	1c x 300mm ²	7
60-ET-19020B	60-EN-19020B	50	BFOU 0.6/1(1.2)kV P5/P12	1c x 300mm ²	7
60-ET-19010A	60-EN-19010A	50	BFOU 0.6/1(1.2)kV P5/P12	1c x 300mm ²	7
60-ET-19010B	60-EN-19010B	50	BFOU 0.6/1(1.2)kV P5/P12	1c x 300mm ²	7
60-EN-19010A	60-ET-19011A	50	BFOU 0.6/1(1.2)kV P5/P12	1c x 300mm ²	1
60-EN-19010B	60-ET-19011B	50	BFOU 0.6/1(1.2)kV P5/P12	1c x 300mm ²	1
60-ET-19011A	60-EL-19011A	50	BFOU 0.6/1(1.2)kV P5/P12	1c x 185mm ²	2
60-ET-19011B	60-EL-19011B	50	BFOU 0.6/1(1.2)kV P5/P12	1c x 185mm ²	2
60-EN-19020A	60-ET-19021A	50	BFOU 0.6/1(1.2)kV P5/P12	1c x 300mm ²	1
60-EN-19020B	60-ET-19021B	50	BFOU 0.6/1(1.2)kV P5/P12	1c x 300mm ²	1
60-ET-19021A	60-EL-19021A	50	BFOU 0.6/1(1.2)kV P5/P12	1c x 185mm ²	2
60-ET-19021B	60-EL-19021B	50	BFOU 0.6/1(1.2)kV P5/P12	1c x 185mm ²	2
60-EN-19010B	60-EN-19020B	50	BFOU 0.6/1(1.2)kV P5/P12	1c x 300mm ²	2
60-EN-19020A	60-EN-19013	50	BFOU 0.6/1(1.2)kV P5/P12	1c x 300mm ²	1
60-EN-19020A	60-EU-19090A	50	BFOU 0.6/1(1.2)kV P5/P12	3c x 120mm ²	-
60-EN-19013	60-EU-19090A	50	BFOU 0.6/1(1.2)kV P5/P12	3c x 120mm ²	-
60-EN-19013	60-EU-19090B	50	BFOU 0.6/1(1.2)kV P5/P12	3c x 120mm ²	-
60-EN-19020B	60-EU-19090B	50	BFOU 0.6/1(1.2)kV P5/P12	3c x 120mm ²	-
60-EN-19020A	60-ET-19008	50	BFOU 0.6/1(1.2)kV P5/P12	1c x 300mm ²	1

4.2.3 PFS Modeling

The PFS have been modeled in two different ways depending on whether the fault is located on the 11kV network or on the secondary side of a transformer. Thus, for short-circuit calculations at high voltage switchboards, the PFS is modeled with a maximum short circuit current $I_k'' = 6800A$. For the low voltage switchboards, the PFS is modeled as an infinite grid with short-circuit power, $S_k'' = 100\ 000\ 000MVA$. The PFS will try to maintain the nominal voltage at the 11kV bus at all times, exceptions are when cases occur that will make the PFS go into a current limiting mode. If a fault occurs on the secondary side of a 690V transformer, the current can get relatively high, and it must be ascertained that it does not cause PFS to go into limiting mode. Theoretically, the PFS will be capable of maintaining the nominal voltage. According to RMS simulations done on PFS, the way of modeling the PFS, as done in this master thesis, is valid and an acceptable approach. [35]

4.2.4 Breaking and Making Capacity

Table 4.6 lists the defined breaking and making capacity limits for maximum short-circuit current at the different voltage-level switchboards. The making capacity will be compared to the maximum peak short-circuit current i_p . The braking capacity will be compared to the 3-cycle braking current, I_b , for the HV switchgear. For the LV switchgear, the braking capacity will be compared to the initial symmetrical short-circuit current I_k'' . It is assumed that the duration of short-circuit, t_k , is 1s. In addition to the breaking and making capacity limits,

Table 4.6: Breaking and making capacities for the different voltage-levels

Voltage [V]	Making capacity [kA]	Breaking capacity [kA]
>1000	100	40
690	143	65
400/230	63	30

NORSOK E-001:2016, states that the maximum initial short-circuit current, I_k'' , should not exceed the values listed in Table 4.7 [36].

Table 4.7: NORSOK E-001:2016 requirements for maximum I_k''

Voltage [V]	Max I_k'' [kA]
>1000	40
690	50
400/230 main distribution boards	30
400/230 sub distribution boards	10

4.2.5 Minimum Short-Circuit

The values from the minimum short-circuit current cases will be compared to the rated current I_r . This rated current gives an indication of which current setting for an inverse time overcurrent protection function could be set.

Table 4.8: Rated current to be compared with minimum short-circuit calculations

Switchboard	U_n [kV]	I_r [kA]	Description
60-EH-19000A	11	1.6	PWP Feeder A current carrying capacity
60-EH-19000B	11	1.6	PWP Feeder B current carrying capacity
60-EH-19001	20	0.058	11/20kV 2 MVA transformer
60-EN-19010A	0.69	2.64	11/0.69kV 3.15 MVA transformer
60-EN-19010B	0.69	2.64	11/0.69kV 3.15 MVA transformer
60-EN-19020A	0.69	2.64	11/0.69kV 3.15 MVA transformer
60-EN-19020B	0.69	2.64	11/0.69kV 3.15 MVA transformer
60-EN-19013	0.69	1.0	SwBd feeder current carrying capacity
60-EL-19011A	0.4	0.7	0.69/0.4kV 0.5 MVA transformer
60-EL-19011B	0.4	0.7	0.69/0.4kV 0.5 MVA transformer
60-EL-19021A	0.4	0.7	0.69/0.4kV 0.5 MVA transformer
60-EL-19021B	0.4	0.7	0.69/0.4kV 0.5 MVA transformer
60-EL-19013A	0.4	0.36	0.69/0.4kV 0.25 MVA transformer
60-EL-19008	0.44	0.67	0.69/0.44kV 0.5 MVA transformer

If the rated current is not noted in the data sheets, it can be derived from Equation 4.2, where U_n is the nominal voltage and S_{rT} is the rated apparent power of the transformer.

$$I_r = \frac{S_{rT}}{\sqrt{3} \times U_n} \quad (4.2)$$

4.3 Case Study

As mentioned in Chapter 4.2.3, the modeling of the PFS for short circuit currents on the HV and LV switchboards differs, and therefore the cases are split into different cases, even though the opening and closing status of the bus-ties will be the same. For all the cases, the essential generator 60-EG-19102 is running.

The original plan was to conduct case studies for different operation scenarios like emergency and essential operating modes, but as stated in Chapter 1.4, this was not completed. The focus of the case study will therefore be on Normal operating mode where the platform is entirely fed by PFS. Different combinations of open and closed bus-ties effect on the short-circuit current will be examined.

For maximum short circuit analysis, only the three-phase short circuit condition is considered. This is because a three-phase fault typically results in the highest fault current magnitude. By analyzing the worst-case scenario of a three-phase fault, one can ensure that the protective devices and equipment are designed to handle the maximum fault current. A c-factor of 1.1 is used for HV switchboards and 1.05 for LV switchboards.

Conversely, when conducting a minimum short-circuit analysis, it is customary to evaluate various fault types in order to ascertain the lowest possible magnitude of fault current. This undertaking holds significant importance in guaranteeing that the protective devices employed within the system are sufficiently sensitive to detect and promptly clear even the most minor faults. For the minimum short-circuit analysis, three-phase short-circuit and phase-to-ground short-circuit will be considered. A c-factor of 1.0 is used for HV switchboards and 0.95 for LV switchboards.

Maximum short-circuit currents

- **Case 1:** Maximum short-circuit on the HV switchboards. Closed bus-ties between 11kV switchboards (60-EH-19000A & 60-EH-19000B), 690V Process Switchboards (60-EN-19010A & 60-EN-19010B) and 690V Utility Switchboard (60-EN-19020A & 60-EN-19020B)
- **Case 2:** Maximum short-circuit on the LV switchboards. Closed bus-ties between 11kV switchboards (60-EH-19000A & 60-EH-19000B), 690V Process Switchboards (60-EN-19010A & 60-EN-19010B) and 690V Utility Switchboard (60-EN-19020A & 60-EN-19020B)
- **Case 2:** Maximum short-circuit on the HV switchboards. Closed bus-ties between 11kV switchboards (60-EH-19000A & 60-EH-19000B), 690V Process Switchboards (60-EN-19010A & 60-EN-19010B) and 690V Utility Switchboard (60-EN-19020A & 60-EN-19020B)
- **Case 4:** Maximum short-circuit on the LV switchboards. Open bus-ties between 11kV switchboards (60-EH-19000A & 60-EH-19000B), 690V Process Switchboards (60-EN-19010A & 60-EN-19010B) and 690V Utility Switchboard (60-EN-19020A & 60-EN-19020B)

- **Case 5:** Maximum short-circuit on the HV switchboards. Open bus-ties between 11kV switchboards (60-EH-19000A & 60-EH-19000B) and 690V Utility Switchboard (60-EN-19020A & 60-EN-19020B). Closed bus tie between 690V Process Switchboards (60-EN-19010A & 60-EN-19010B).
- **Case 6:** Maximum short-circuit on the LV switchboards. Open bus-ties between 11kV switchboards (60-EH-19000A & 60-EH-19000B) and 690V Utility Switchboard (60-EN-19020A & 60-EN-19020B). Closed bus tie between 690V Process Switchboards (60-EN-19010A & 60-EN-19010B).

Minimum short-circuit currents

- Case 7: Minimum short-circuit on the HV switchboards. Closed bus-ties between 11kV switchboards (60-EH-19000A & 60-EH-19000B), 690V Process Switchboards (60-EN-19010A & 60-EN-19010B) and 690V Utility Switchboard (60-EN-19020A & 60-EN-19020B)
- Case 8: Minimum short-circuit on the LV switchboards. Closed bus-ties between 11kV switchboards (60-EH-19000A & 60-EH-19000B), 690V Process Switchboards (60-EN-19010A & 60-EN-19010B) and 690V Utility Switchboard (60-EN-19020A & 60-EN-19020B)
- Case 9: Minimum short-circuit on the HV switchboards. Open bus-ties between 11kV switchboards (60-EH-19000A & 60-EH-19000B), 690V Process Switchboards (60-EN-19010A & 60-EN-19010B) and 690V Utility Switchboard (60-EN-19020A & 60-EN-19020B)
- Case 10: Minimum short-circuit on the LV switchboards. Open bus-ties between 11kV switchboards (60-EH-19000A & 60-EH-19000B), 690V Process Switchboards (60-EN-19010A & 60-EN-19010B) and 690V Utility Switchboard (60-EN-19020A & 60-EN-19020B)

4.4 Short-Circuit Calculation

The maximum and minimum short-circuit calculations are performed according to IEC 60909. As mentioned, the Valhall field and platforms are powered from shore, through a HVDC cable which leads to the need of conducting the short-circuit calculations in two rounds, however, the calculation settings will be the same for both the HV and LV switchboards. Table 4.9 shows the calculation settings for the maximum short-circuit calculations. Table 4.10 shows the calculation settings for the minimum short-circuit calculations.

Table 4.9: Calculation settings for maximum short-circuit

Calculation type	Maximum short circuit
Method	IEC 60909
LV tolerance	6%
C-factor c-factor	Standard defined table
Breaking Time	0.10s
Fault Clearing Time (I_{th})	1.00s
Fault Impedance	0.0 Ω
Grid Identification	Automatic
Cable Temperature	20°C
Asynchronous motors	Always considered
Peak Short-Circuit Current (i_p)	Method C(1)
Decaying Aperiodic Component (i_{dc})	Method B
Calculate Ik	Ignore Motor Contributions

Table 4.10: Calculation settings for minimum short-circuit

Calculation type	Minimum short circuit
Method	IEC 60909
LV tolerance	6%
C-factor c-factor	Standard defined table
Breaking Time	0.10s
Fault Clearing Time (I_{th})	1.00s
Fault Impedance	0.0 Ω
Grid Identification	Automatic
Cable Temperature	20°C
Asynchronous motors	Always considered
Peak Short-Circuit Current (i_p)	Method C(1)
Decaying Aperiodic Component (i_{DC})	Method B
Calculate Ik	Ignore Motor Contributions

4.5 Arc-Flash Analysis

For conducting the arc-flash analysis, IEEE 1584 and its step, as described in Section 3.2.3. Values for working distance, typical busbar gap and enclosure size, i.e. step 4-6, that was planned to be implemented into the model, are shown in Table 4.11. These values are based on IEEE 1584 [9]. This does not apply to the 20kV switchboards (60-EH-19001) as IEEE 1584 only includes nominal voltages up to 15kV.

Table 4.11: Switchboard design

Voltage [V]	Equipment Class	Working dist. [mm]	Busbar gap [mm]	Enclosure Size ($H \times W \times D$) [mm]	Electrode configuration
1100	15 kV Switchgear	914.4	152	$1143 \times 762 \times 762$	HCB
690/440/400	LV Switchgear	609.6	32	$508 \times 508 \times 508$	HCB

Table 4.12 shows the circuit breaker types it is proposed to use in the electrical network and their respective breaking time, and 4.13 shows the proposed arc flash protection unit and the respective relay delay [37], [38].

Table 4.12: Circuit breakers and respective fault clearing time

Voltage [V]	Circuit Breaker Type	Breaking time [ms]
HV (>1000V)	ZS1	60
LV (690V)	E _{max}	70
LV (440/400V)	-	200

Table 4.13: Arc flash protection for 11kV and 690V switchboards

Voltage [V]	Arc Flash Protection	Relay delay [ms]
HV (>1000V)	IED	12
LV (690V)	IED	12
LV (690V)	TVOC	2

Chapter 5

Results and Discussions

In this chapter, the results from the short-circuit analysis will be presented and discussed.

5.1 Short-Circuit Currents

5.1.1 Maximum Short-Circuit Currents

Case 1: HV switchboards and closed bus-ties

For the first case, the maximum short-circuit on the HV switchboards was conducted. The bus-ties was closed between the 11kV switchboards (60-EH-19000A & 60-EH-19000B), 690V Process Switchboards (60-EN-19010A & 60-EN-19010B) and 690V Utility Switchboard (60-EN-19020A & 60-EN-19020B). The results are presented in Table 5.1.

Table 5.1: Results from case 1

Bus	U_n [kV]	Swbrd rating		I_p [kA]	I_k'' [kA]	I_b [kA]
		I_p [kA]	I_k/t_k [kA/1s]			
60-EH-19000A	11	104	40	78.2	34.1	27.2
60-EH-19000B	11	100	40	78.2	34.1	27.2
60-EH-19001	20	100	40	1.627	0.677	1.1

Case 2: LV switchboards and closed bus-ties

For the second case, the maximum short-circuit on the LV switchboards was conducted. The same bus-ties were closed as in case 1. The results are presented in Table 5.2.

Table 5.2: Results from case 2

Bus	U_n [V]	Swbrd rating		3-phase	
		I_p [kA]	I_k/t_k [kA/1s]	I_p [kA]	I_k'' [kA]
60-EN-19010A	690	143	65	110.2	46.5
60-EN-19010B	690	143	65	110.2	46.5
60-EN-19020A	690	143	65	110.2	46.5
60-EN-19020B	690	143	65	110.2	46.5
60-EL-19011A	400	63	30	16.58	8.2
60-EL-19011B	400	63	30	16.58	8.2
60-EL-19021A	400	63	30	16.58	8.2
60-EL-19021B	400	63	30	16.58	8.2
60-EL-19008	440	63	30	20.09	9.9

All the values are within defined limits for initial and peak values. The initial current is also within NORSOK requirements, according to 4.7.

Case 3: HV switchboards with open bus-ties

For the third case, the maximum short-circuit on the HV switchboards was conducted. The bus-ties was opened between 11kV switchboards (60-EH-19000A & 60-EH-19000B), 690V Process Switchboards (60-EN-19010A & 60-EN-19010B) and 690V Utility Switchboard (60-EN-19020A & 60-EN-19020B). The results are presented in Table 5.3.

Table 5.3: Results from case 3

Bus	U_n [kV]	Swbrd rating		I_p [kA]	I_k'' [kA]	I_b [kA]
		I_p [kA]	I_k/t_k [kA/1s]			
60-EH-19000A	11	104	40	76.5	33.1	26.8
60-EH-19000B	11	100	40	76.4	32.9	26.6
60-EH-19001	20	100	40	1.63	0.676	0.676

For case 3, the values were also within limits. The opening of the bus-ties did not really affect the HV values, as expected.

Case 4: LV switchboards with open bus-ties

For the fourth case, the maximum short-circuit on the LV switchboards was conducted. The same bus-ties were open as in case 3. The results are presented in Table 5.4.

Table 5.4: Results from case 4

Bus	U_n [V]	Swbrd rating		3-phase	
		I_p [kA]	I_k/t_k [kA/1s]	I_p [kA]	I_k'' [kA]
60-EN-19010A	690	143	65	67.6	28.86
60-EN-19010B	690	143	65	67.5	28.83
60-EN-19020A	690	143	65	67.6	28.86
60-EN-19020B	690	143	65	67.5	28.83
60-EL-19011A	400	63	30	15.7	7.7
60-EL-19011B	400	63	30	15.7	7.7
60-EL-19021A	400	63	30	15.7	7.7
60-EL-19021B	400	63	30	15.7	7.7
60-EL-19008	440	63	30	18.94	9.32

Opening of the bus-ties resulted in lower values for the 690V switchboards compared to the results from case 2 in Table 5.1. The values for I_p and I_k'' are also somewhat reduced compared to case 2. The values are still within rated limits.

Case 5: HV switchboards with closed bus-tie between Process Switchboards (690V)

For the fifth case, the maximum short-circuit on the HV switchboards was conducted. In this case, the only closed bus-tie in the system was between the 690V Process switchboards. (60-EN-19010A and 60-EN-19010A) The results are presented in Table 5.5.

Table 5.5: Results from case 5

Bus	U_n [kV]	Swbrd rating		I_p [kA]	I_k'' [kA]	I_b [kA]
		I_p [kA]	I_k/t_k [kA/1s]			
60-EH-19000A	11	104	40	76.5	33.1	26.8
60-EH-19000B	11	100	40	76.4	32.9	26.6
60-EH-19001	20	100	40	1.62	0.676	0.676

Case 6: LV switchboards with closed bus-ties between Process Switchboards (690V)

For the sixth, and last maximum short-circuit current case, the bus-ties are open as explained in case 5. The results are presented in Table 5.6. For case 6, the occurrence of higher

Table 5.6: Results from case 6

Bus	U_n [V]	Swbrd rating		3-phase	
		I_p [kA]	I_k/t_k [kA/1s]	I_p [kA]	I_k'' [kA]
60-EN-19010A	690	143	65	110.2	46.5
60-EN-19010B	690	143	65	110.2	46.5
60-EN-19020A	690	143	65	67.6	28.9
60-EN-19020B	690	143	65	67.5	28.8
60-EL-19011A	400	63	30	16.6	8.15
60-EL-19011B	400	63	30	16.6	8.15
60-EL-19021A	400	63	30	15.7	7.68
60-EL-19021B	400	63	30	15.7	7.68
60-EL-19008	440	63	30	18.9	9.33

short-circuit currents at closed bus-tie is also applied, as the highest values can be observed at 60-EN-19010A and 60-EN-19010B. The 400V process main distribution boards (60-EL-19011A and 60-EL-19011B), which are fed by the Process switchboards, are also affected by the closed bus-tie. The 3-phase short-circuit values are higher when the bus-tie is closed.

5.1.2 Discussion of the Maximum Short-Circuit Results

The main observation from the maximum short-circuit results is that all the values are within the defined limits for the initial symmetrical short-circuit current I_k'' , which can indicate that the network is designed in an adequate manner.

Another observation of the maximum short-circuit calculations is that whenever a bus-tie is closed between two of the 690-V switchboards, both I_p and I_k'' is large compared to whenever the bus-tie is open. Reasons for this can be the presence of the closed bus tie creates a low-impedance path for the fault current flow. This path likely offers less resistance compared to the alternate paths available when the tie is open. If the bus-tie is closed, it connects the two switchboards, whereas when the bus-tie is open, it splits the switchboards.

Another explanation for the increased values whenever the bus-tie is closed can be mistakes in the model caused by human error. A lot of different inputs were applied to the system and it is possible that human error has impacted the results.

5.1.3 Minimum Short-Circuit Currents

Case 7: HV switchboards and closed bus-ties

Table 5.7 shows the minimum short-circuit currents for the HV switchboards with closed bus-ties between the 11kV switchboards, both 690V process switchboards, and both 690 utility switchboards. The I_r/I_k'' ratio for the different switchboards is also shown in Table 5.7.

Table 5.7: Results from case 7

Bus	Un[kV]	Ir [kA]	Three phase		Line-Line	
			Ik''[kA]	Ik''/Ir	Ik''[kA]	Ik''/Ir
60-EH-19000A	11	1.6	1.98	1.23	1.7	1.06
60-EH-19000B	11	1.6	1.98	1.23	1.7	1.06
60-EH-19001	20	0.058	0.43	7.4	0.375	6.46

Case 8: LV switchboards and closed bus-ties

Table 5.8 shows the minimum short-circuit currents for the LV switchboards where the same bus-ties are closed as in case 7 . between both the 690V process switchboards and both 690 utility switchboards. The I_r/I_k'' ratio for the different switchboards is also shown in Table 5.8.

Table 5.8: Results from case 8

Bus	Un[V]	Ir [kA]	Three phase		Line-Line	
			Ik''[kA]	Ik''/Ir	Ik''[kA]	Ik''/Ir
60-EN-19010A	690	2.64	20.6	7.8	17.8	6.7
60-EN-19010B	690	2.64	20.6	7.8	17.8	6.7
60-EN-19020A	690	2.64	20.6	7.8	17.8	6.7
60-EN-19020B	690	2.64	20.6	7.8	17.8	6.7
60-EL-19011A	400	0.7	6.5	9.29	5.63	8
60-EL-19011B	400	0.7	6.5	9.29	5.63	8
60-EL-19021A	400	0.7	6.5	9.29	5.63	8
60-EL-19021B	400	0.7	6.5	9.29	5.63	8
60-EL-19008	440	0.67	6	8.955	6.8	10.1

Case 9: HV switchboards and open bus-ties

For case 9, the minimum short-circuit current for HV switchboards with all bus-ties open was calculated. The values are presented in Table 5.9 along with the ratio between the short circuit current and the defined current rating I_r/I_k'' .

Table 5.9: Results from case 9

Bus	Un[kV]	Ir [kA]	Three phase		Line-Line	
			Ik''[kA]	Ik''/Ir	Ik''[kA]	Ik''/Ir
60-EH-19000A	11	1.6	1.98	1.2	1.7	1.06
60-EH-19000B	11	1.6	1.97	1.2	1.7	1.06
60-EH-19001	20	0.058	0.43	7.4	0.375	6.46

Case 10: LV switchboards and open bus-ties

For case 10, the minimum short-circuit current for LV switchboards with all bus-ties open was calculated. The values are presented in Table 5.10 along with the ratio between the short circuit current and the defined current rating I_r/I_k'' .

Table 5.10: Results from case 10

Bus	Un[V]	Ir [kA]	Three phase		Line-Line	
			Ik''[kA]	Ik''/Ir	Ik''[kA]	Ik''/Ir
60-EN-19010A	690	2.64	15.7	5.94	13.6	5.15
60-EN-19010B	690	2.64	15.7	5.94	13.6	5.15
60-EN-19020A	690	2.64	15.7	5.94	13.6	5.15
60-EN-19020B	690	2.64	15.7	5.94	13.6	5.15
60-EL-19011A	400	0.7	6.15	8.78	5.3	7.57
60-EL-19011B	400	0.7	6.15	8.78	5.3	7.57
60-EL-19021A	400	0.7	6.15	8.78	5.3	7.57
60-EL-19021B	400	0.7	6.15	8.78	5.3	7.57
60-EL-19008	440	0.67	7.43	11.1	6.4	9.55

5.1.4 Discussion of the Minimum Short-Circuit Results

For the minimum short circuit results, the same observation regarding the relationship between the opening and closing of bus-ties and the value of the short-circuit currents in the LV switchboards. For case 9, I_k'' is larger than in case 11. This applies for both fault types, both three-phase and Line-Line.

The I_r/I_k'' -ratio shows that short-circuit currents are above the respective transformer rated current and feeder cables current carrying capacity.

Overall, after conducting a short-circuit calculation for the network in normal operation mode for different scenarios, the results showed that the short-circuit currents fall within the defined limits of the network. This indicates that the network is operating within its expected parameters and is capable of handling potential short-circuit scenarios without compromising safety. This adherence to limits is crucial in maintaining the stability and reliability of the network, as exceeding these limits could lead to equipment damage, power outages, or even pose safety hazards.

Chapter 6

Conclusions and Further Work

In this chapter, the most important aspects of the thesis is presented, as well as recommendations for future work.

In this thesis, the modeling and analysis of an electrical network of an offshore oil and gas platform in the software PowerFactory by DIgSILENT was performed. The modeled platform is a production and wellhead platform that will be joined to the Valhall field, which is supplied with PFS. A big and time-consuming part of the thesis was to model the network, consisting of 14 switchboards, 13 transformers, PFS-modeling, and numerous HV and LV cables, amongst others.

A short-circuit analysis was performed according to IEC 60909. Various cases where different combinations of open and closed bus-ties between 690V switchboards and 11kV switchboards were examined for both maximum and minimum short-circuit calculations. The maximum short-circuit current was used to ensure compliance with switchgear ratings and the minimum short-circuit current was calculated for protective device coordination. The results suggest that the maximum short-circuit current complies with the switchgear ratings, i.e. making and braking capacity, for all switchboards at PWP. For the minimum short-circuit calculations, the ratio between the rated current of the respective transformer or feeder cable of the switchboard to the initial symmetrical short-circuit current, I_r/I_k'' was calculated as well. For all switchboards, the ratio was adequately high.

Further work

Due to a lot of difficulties regarding the model in DIgSILENT PowerFactory, the scope had to be reduced. Therefore the analysis can be developed further. The following steps can be proposed to be done as further work:

- **Implement arc-flash protection units into the model:** Following up on the model for conducting the arc-flash analysis according to IEEE 1584.
- **Expand the analysis operation modes:** The short circuit calculations and arc-flash analysis could be done for essential and emergency modes as well. For essential mode, the PFS is shut down, and the field is supplied from essential generators at PH and PWP. For Emergency mode, the emergency switchboards will be fed from emergency generators at PH and IP. For both these operation modes, it would be of interest to conduct short-circuit calculations and arc-flash calculations for different scenarios, including worst-case scenario.
- **Conduct other types of power system analysis:** This could include load flow, harmonic analysis, dynamic analysis and transient analysis to further ensure safe, reliable and efficient operation of the power system.

Bibliography

- [1] Miljøstatus by Miljødirektoratet. *Klimagassutslipp fra olje- og gassutvinning i Norge*. Last accessed 04.06.2023. 2022. URL: <https://miljostatus.miljodirektoratet.no/tema/klima/norske-utslipp-av-klimagasser/klimagassutslipp-fra-olje--og-gassutvinning/>.
- [2] Aker BP. *Valhall PWP-Fenris*. Last accessed 23.05.2023. 2022. URL: <https://akerbp.com/project/valhall-pwp-fenris/>.
- [3] Norsk Oljemuseum. *Olje- og gassfelt i Norge*. Last accessed 25.05.2023. 2016. URL: <https://www.norskolje.museum.no/wp-content/uploads/2017/06/006-Valhallomr%5C%C3%5C%A5det-fra-2012-0lje-og-gassfelt-i-Norge-.pdf>.
- [4] Equinor. *Johan Sverdrup*. Last accessed 04.06.2023. URL: <https://www.equinor.com/energy/johan-sverdrup>.
- [5] Nasser Tleis. “Power Systems Modelling and Fault Analysis.” In: *Power Systems Modelling and Fault Analysis* (Jan. 2008). DOI: [10.1016/B978-0-7506-8074-5.X5001-2](https://doi.org/10.1016/B978-0-7506-8074-5.X5001-2).
- [6] “Recommended Practice for Calculating AC Short-Circuit Currents in Industrial and Commercial Power Systems.” In: *IEEE Std 551-2006 [The Violet Book]* (2006), pp. 1–308. DOI: [10.1109/IEEESTD.2006.248693](https://doi.org/10.1109/IEEESTD.2006.248693).
- [7] J.C. Das. *Arc Flash Hazard Analysis and Mitigation*. Dec. 2020. ISBN: 9781119709787. DOI: [10.1002/9781119709787](https://doi.org/10.1002/9781119709787).
- [8] International Electrotechnical Commission. “IEC 60909-0 Short-circuit currents in three-phase a.c.systems - Part 0: Calculation of currents.” In: 2.0 (2016), pp. 1–154.
- [9] “IEEE Guide for Performing Arc-Flash Hazard Calculations.” In: *IEEE Std 1584-2018 (Revision of IEEE Std 1584-2002)* (2018), pp. 1–134. DOI: [10.1109/IEEESTD.2018.8563139](https://doi.org/10.1109/IEEESTD.2018.8563139).
- [10] Kiing Ing Wong et al. “Analysis of Electrical Distribution System for Offshore Oil and Gas Platform.” In: *2019 IEEE Asia Power and Energy Engineering Conference (APEEC)*. 2019, pp. 302–306. DOI: [10.1109/APEEC.2019.8720690](https://doi.org/10.1109/APEEC.2019.8720690).
- [11] K.N. Hasan, K. S. R. Rao, and Z. Mokhtar. “Analysis of load flow and short circuit studies of an offshore platform using ERACS software.” In: *2008 IEEE 2nd International Power and Energy Conference*. 2008, pp. 543–548. DOI: [10.1109/PECON.2008.4762535](https://doi.org/10.1109/PECON.2008.4762535).
- [12] Zaw Aung and Aung Latt. “Short Circuit Analysis of 33/11/0.4 kV Distribution System Using ETAP.” In: (May 2019).
- [13] Guanbiao Huang et al. “Short Circuit Current Algorithm and Software Design Based on IEC60909 Standard.” In: 2418.1 (Feb. 2023), p. 012113. DOI: [10.1088/1742-6596/2418/1/012113](https://doi.org/10.1088/1742-6596/2418/1/012113). URL: <https://dx.doi.org/10.1088/1742-6596/2418/1/012113>.
- [14] Kadir Ozen et al. “Arc-Flash Risk Level Calculations based on Computer Simulations and Measures to Avoid Hazards.” In: *2018 20th International Symposium on Electrical Apparatus and Technologies (SIELA)*. 2018, pp. 1–4. DOI: [10.1109/SIELA.2018.8447123](https://doi.org/10.1109/SIELA.2018.8447123).
- [15] Adam Reeves, Mark Freyenberger, and Michael Hodder. “Understanding the Effect of Electrode Configuration on Incident Energy and Arc-Flash Boundary.” In: *IEEE Transactions on Industry Applications* 56.6 (2020), pp. 6069–6075. DOI: [10.1109/TIA.2020.3023918](https://doi.org/10.1109/TIA.2020.3023918).
- [16] DIgSILENT GmbH. *PowerFactory 2023 User Manual*. English. Version 2023. DIgSILENT. Feb. 2, 2023. 1482 pp. In press.

- [17] B. de Metz-Noblat, F. Dumas, C. Poulain. *Cahier technique no. 158: Calculation of short-circuit currents*. Last accessed 25.04.2023. 2005.
- [18] Dusko Nedic et al. "A COMPARISON OF SHORT CIRCUIT CALCULATION METHODS AND GUIDELINES FOR DISTRIBUTION NETWORKS." In: *19th International Conference on Electricity Distribution* (2007), pp. 1–4.
- [19] Yuhong Zhang et al. "The adaptability of IEC 60909: 0-2016 to power grid with voltage levels above 400kV." In: *Journal of Physics: Conference Series* 2276 (May 2022). DOI: [10.1088/1742-6596/2276/1/012018](https://doi.org/10.1088/1742-6596/2276/1/012018).
- [20] Rade Ciric. *Lecture notes in High Voltage - Fault analysis by coupling component systems at the fault point*.
- [21] Konrad Schmitt et al. "Short Circuit and Arc Flash Study on a Microgrid Facility." In: 3 (May 2021), pp. 14–23.
- [22] Adam Reeves, Mark Freyenberger, and Michael Hodder. "Understanding the Effect of Electrode Configuration on Incident Energy and Arc-Flash Boundary." In: *IEEE Transactions on Industry Applications* 56.6 (2020), pp. 6069–6075. DOI: [10.1109/TIA.2020.3023918](https://doi.org/10.1109/TIA.2020.3023918).
- [23] etap. *IEEE 1584-2018 Arc Flash Incident Energy Calculation*. URL: <https://etap.com/arc-flash/arc-flash-ieee1584-2018>.
- [24] "NFPA 70E: Standard for Electrical Safety in the Workplace 2015 Edition." In: *NFPA Std.* (2015).
- [25] Aker Solutions. *Electrical Load List -PWP*. March 2023.
- [26] Aker Solutions. *HV TRANSFORMER DATA SHEETS - PWP*. Dec 2022.
- [27] Aker Solutions. *HV 20KV TRANSFORMER DATA SHEET - PWP*. Dec 2022.
- [28] Aker Solutions. *HV 11KV SWITCHGEAR DATA SHEET - PWP*. Dec 2022.
- [29] Aker Solutions. *LV 690V SWITCHGEAR DATA SHEET - PWP*. Jan 2023.
- [30] Aker BP. *Power system philosophy - PWP/FEN*. Jan 2023.
- [31] Unitech Power Systems AS. *Valhall PWP FEED study*. Aug. 2022.
- [32] Draka. *FlexFlame RFOU 6/10(12)kV P3/P10 Power Cable Catalog*. Sep 2022.
- [33] Draka. *FlexFlame RFOU 12/20(24)kV P19/P21 Power Cable Catalog*. Sep 2022.
- [34] Draka. *FlexFlame BFOU 0.6/1(1.2)kV P5/P12 Power Cable Catalog*. June 2018.
- [35] Unitech. *Valhall Complex/Lista - As Built Power System Study*. May 2023.
- [36] Norsok standard. *NORSOK E-001:2016 ed.6, "Electrical Systems"*. Last accessed 04.06.2023. 2016.
- [37] ABB. *UniGear ZS1 Medium-voltage air-insulated switchgear up to 24 kV*. Last accessed 04.06.2023.
- [38] ABB. *SACE Emax Low voltage air circuit-breakers*. Last accessed 04.06.2023.

Appendix A

Coefficients for arc-flash hazard analysis

A.1 Coefficients for calculating arcing current

E.C. / V_{ec}		k_1	k_2	k_3	k_4	k_5	k_6	k_7	k_8	k_9	k_{10}
VCB	600 V	-0.04287	1.035	-0.083	0	0	-4.783E-09	1.962E-06	-0.000229	0.003141	1.092
	2 700 V	0.0065	1.001	-0.024	-1.557E-12	4.556E-10	-4.186E-08	8.346E-07	5.482E-05	-0.003191	0.9729
	14 300 V	0.005795	1.015	-0.011	-1.557E-12	4.556E-10	-4.186E-08	8.346E-07	5.482E-05	-0.003191	0.9729
VCBB	600 V	-0.017432	0.98	-0.05	0	0	-5.767E-09	2.524E-06	-0.00034	0.01187	1.013
	2 700 V	0.002823	0.995	-0.0125	0	-9.204E-11	2.901E-08	-3.262E-06	0.0001569	-0.004003	0.9825
	14 300 V	0.014827	1.01	-0.01	0	-9.204E-11	2.901E-08	-3.262E-06	0.0001569	-0.004003	0.9825
HCB	600 V	0.054922	0.988	-0.11	0	0	-5.382E-09	2.316E-06	-0.000302	0.0091	0.9725
	2 700 V	0.001011	1.003	-0.0249	0	0	4.859E-10	-1.814E-07	-9.128E-06	-0.0007	0.9881
	14 300 V	0.008693	0.999	-0.02	0	-5.043E-11	2.233E-08	-3.046E-06	0.000116	-0.001145	0.9839
VOA	600 V	0.043785	1.04	-0.18	0	0	-4.783E-09	1.962E-06	-0.000229	0.003141	1.092
	2 700 V	-0.02395	1.006	-0.0188	-1.557E-12	4.556E-10	-4.186E-08	8.346E-07	5.482E-05	-0.003191	0.9729
	14 300 V	0.005371	1.0102	-0.029	-1.557E-12	4.556E-10	-4.186E-08	8.346E-07	5.482E-05	-0.003191	0.9729
HOA	600 V	0.111147	1.008	-0.24	0	0	-3.895E-09	1.641E-06	-0.000197	0.002615	1.1
	2 700 V	0.000435	1.006	-0.038	0	0	7.859E-10	-1.914E-07	-9.128E-06	-0.0007	0.9981
	14 300 V	0.000904	0.999	-0.02	0	0	7.859E-10	-1.914E-07	-9.128E-06	-0.0007	0.9981

Figure A.1: Coefficients for Equation 3.21 [9]

A.2 Coefficients for calculating incident energy

600 V	k_1	k_2	k_3	k_4	k_5	k_6	k_7	k_8	k_9	k_{10}	k_{11}	k_{12}	k_{13}
VCB	0.753364	0.566	1.752636	0	0	-4.783E-09	0.000001962	-0.000229	0.003141	1.092	0	-1.598	0.957
VCBB	3.068459	0.26	-0.098107	0	0	-5.767E-09	0.000002524	-0.00034	0.01187	1.013	-0.06	-1.809	1.19
HCB	4.073745	0.344	-0.370259	0	0	-5.382E-09	0.000002316	-0.000302	0.0091	0.9725	0	-2.03	1.036
VOA	0.679294	0.746	1.222636	0	0	-4.783E-09	0.000001962	-0.000229	0.003141	1.092	0	-1.598	0.997
HOA	3.470417	0.465	-0.261863	0	0	-3.895E-09	0.000001641	-0.000197	0.002615	1.1	0	-1.99	1.04

2700 V	k_1	k_2	k_3	k_4	k_5	k_6	k_7	k_8	k_9	k_{10}	k_{11}	k_{12}	k_{13}
VCB	2.40021	0.165	0.354202	-1.557E-12	4.556E-10	-4.186E-08	8.346E-07	5.482E-05	-0.003191	0.9729	0	-1.569	0.9778
VCBB	3.870592	0.185	-0.736618	0	-9.204E-11	2.901E-08	-3.262E-06	0.0001569	-0.004003	0.9825	0	-1.742	1.09
HCB	3.486391	0.177	-0.193101	0	0	4.859E-10	-1.814E-07	-9.128E-06	-0.0007	0.9881	0.027	-1.723	1.055
VOA	3.880724	0.105	-1.906033	-1.557E-12	4.556E-10	-4.186E-08	8.346E-07	5.482E-05	-0.003191	0.9729	0	-1.515	1.115
HOA	3.616266	0.149	-0.761561	0	0	7.859E-10	-1.914E-07	-9.128E-06	-0.0007	0.9981	0	-1.639	1.078

14 300 V	k_1	k_2	k_3	k_4	k_5	k_6	k_7	k_8	k_9	k_{10}	k_{11}	k_{12}	k_{13}
VCB	3.825917	0.11	-0.999749	-1.557E-12	4.556E-10	-4.186E-08	8.346E-07	5.482E-05	-0.003191	0.9729	0	-1.568	0.99
VCBB	3.644309	0.215	-0.585522	0	-9.204E-11	2.901E-08	-3.262E-06	0.0001569	-0.004003	0.9825	0	-1.677	1.06
HCB	3.044516	0.125	0.245106	0	-5.043E-11	2.233E-08	-3.046E-06	0.000116	-0.001145	0.9839	0	-1.655	1.084
VOA	3.405454	0.12	-0.93245	-1.557E-12	4.556E-10	-4.186E-08	8.346E-07	5.482E-05	-0.003191	0.9729	0	-1.534	0.979
HOA	2.04049	0.177	1.005092	0	0	7.859E-10	-1.914E-07	-9.128E-06	-0.0007	0.9981	-0.05	-1.633	1.151

Figure A.2: Coefficients for Equation 3.22 [9]